Name of the Teacher: DR. SUBHANKAR SARDAR
Class: Semester-6
Paper: C14T (Physical Chemistry)
Topic: Molecular Spectroscopy (Raman spectroscopy, NMR and ESR)

Comments: Read as much as you can. The highlighted and the quoted portions are must read.

Reference: Fundamentals of molecular spectroscopy by C.N. Banwell

CHAPTER
FOUR

RAMAN SPECTROSCOPY

4.1 INTRODUCTION

When a beam of light is passed through a transparent substance, a small amount of the radiation energy is scattered, the scattering persisting even if all dust particles or other extraneous matter are rigorously excluded from the substance. If monochromatic radiation, or radiation of a very narrow frequency band, is used, the scattered energy will consist almost entirely of radiation of the incident frequency (the so-called *Rayleigh scattering*) but, in addition, certain discrete frequencies above and below that of the incident beam will be scattered; it is this which is referred to as *Raman scattering*.

4.1.1 Quantum Theory of Raman Effect

The occurrence of Raman scattering may be most easily understood in terms of the quantum theory of radiation. This treats radiation of frequency ν as consisting of a stream of particles (called photons) having energy $h\nu$ where h is Planck's constant. Photons can be imagined to undergo collisions with molecules and, if the collision is perfectly elastic, they will be deflected unchanged. A detector placed to collect energy at right angles to an incident beam will thus receive photons of energy $h\nu$, i.e. radiation of frequency ν. Elastic scattering can be likened to a ball bearing striking a rigid table—the ball bearing bounces off the table without any loss of energy.

However, it may happen that energy is exchanged between photon and molecule during the collision: such collisions are called 'inelastic'. The molecule can gain or lose amounts of energy only in accordance with the quantal laws; i.e. its energy change, ΔE joules, must be the difference in energy between two of its allowed states. That is to say, ΔE must represent a change in the vibrational and/or rotational energy of the molecule. If the molecule *gains* energy ΔE, the photon will be scattered with energy $h\nu - \Delta E$ and the equivalent radiation will have a frequency $\nu - \Delta E/h$. Conversely, if the molecule *loses* energy ΔE, the scattered frequency will be $\upsilon + \Delta E/h$. The inelastic process can be pictured in terms of a ball bearing striking a drum. If the surface of the drum is stationary when the ball bearing hits, it will start oscillating at its own

normal frequency and the ball bearing will be reflected with less energy, having lost an amount of energy equal to that taken up by the oscillation of the drum. On the other hand, if the drum is already oscillating when the ball bearing strikes, and if the ball bearing hits at the right phase of the drum's oscillation, the drum will give energy to the ball bearing—rather like a catapult—and the ball bearing will be flung off with increased energy.

Radiation scattered with a frequency lower than that of the incident beam is referred to as Stokes' radiation, while that at higher frequency is called anti-Stokes' radiation. Since the former is accompanied by an *increase* in molecular energy (which can always occur, subject to certain selection rules) while the latter involves a *decrease* (which can only occur if the molecule is originally in an excited vibrational or rotational state), Stokes' radiation is generally more intense than anti-Stokes' radiation. Overall, however, the total radiation scattered at any but the incident frequency is extremely small, and sensitive apparatus is needed for its study.

4.1.2 Classical Theory of the Raman Effect: Molecular Polarizability

The classical theory of the Raman effect, while not wholly adequate, is worth consideration since it leads to an understanding of a concept basic to this form of spectroscopy—the polarizability of a molecule. When a molecule is put into a static electric field it suffers some distortion, the positively charged nuclei being attracted towards the negative pole of the field, the electrons to the positive pole. This separation of charge centres causes an *induced electric dipole moment* to be set up in the molecule and the molecule is said to be *polarized*. The size of the induced dipole μ, depends both on the magnitude of the applied field, E, and on the ease with which the molecule can be distorted. We may write

$$\mu = \alpha E \tag{4.1}$$

where α is the *polarizability* of the molecule.

Consider first the diatomic molecule H_2, which we show placed in an electric field in Fig. 4.1(*a*) and (*b*) in end-on and sideways orientation, respectively. The electrons forming the bond are more easily displaced by the field *along* the bond axis (Fig. 4.1(*b*)) than that *across* the bond (Fig. 4.1(*a*)), and the polarizability is thus said to be *anisotropic*. This fact may be confirmed

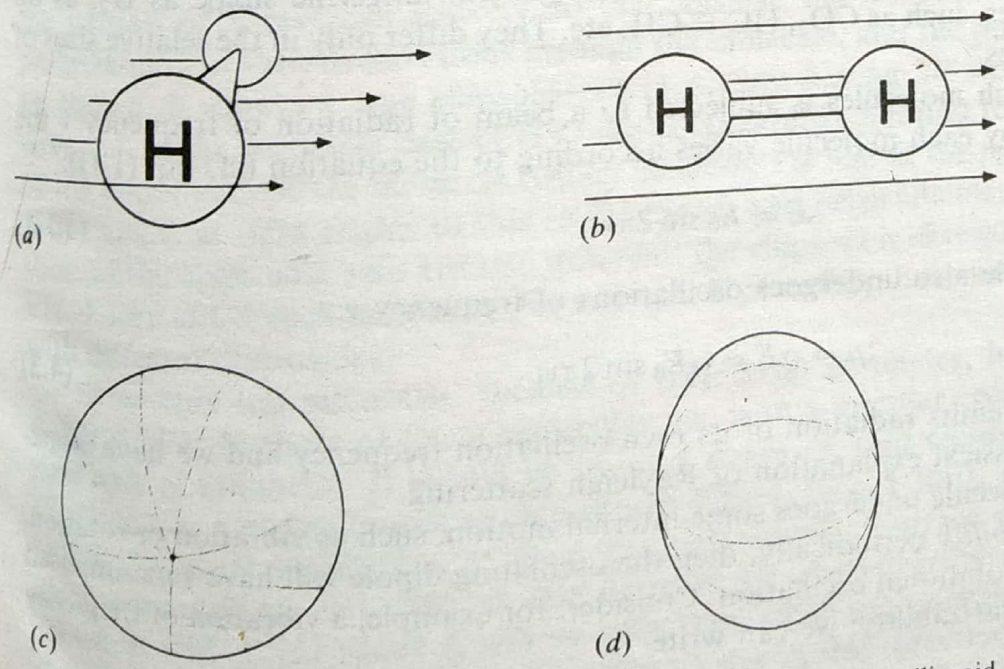

Figure 4.1 The hydrogen molecule in an electric field and its polarizability ellipsoid, seen along and across the bond axis.

experimentally (e.g. by a study of the intensity of lines in the Raman spectrum of H_2), when it is found that the induced dipole moment for a given field applied along the axis is approximately twice as large as that induced by the same field applied across the axis; fields in other directions induce intermediate dipole moments.

The polarizability of a molecule in various directions is conventionally represented by drawing a *polarizability ellipsoid*. We shall define this formally in the next paragraph, but for hydrogen its general shape is that of a squashed sphere, like a tangerine, and we have drawn this in two orientations in Fig. 4.1(*c*) and (*d*) (together with totally imaginary tangerine segment lines to make the picture clearer). In Fig. 4.1(*c*) we are looking down on to the top of the tangerine just off its axis and in Fig. 4.1(*d*) we look at it sideways; these viewpoints correspond to those for the hydrogen molecule in Fig. 4.1(*a*) and (*b*), respectively.

In general a polarizability ellipsoid is defined as a three-dimensional surface whose distance from the electrical centre of the molecule (in H_2 this is also the centre of gravity) is proportional to $1/\sqrt{a_i}$, where a_i is the polarizability along the line joining a point i on the ellipsoid with the electrical centre. Thus where the polarizability is *greatest*, the axis of the ellipsoid is *least*, and vice versa. (Historically this representation arose by analogy with the momentum of a body—the momental ellipsoid is defined similarly using $1/\sqrt{I_i}$, where I_i is the moment of inertia about an axis i.)

If we imagine applying an electric field across the bond axis of H_2, as in Fig. 4.1(*a*), a certain amount of polarization of the molecule will occur. If we also imagine the molecule rotating about its bond axis, it is obvious that it will present exactly the same aspect to the electric field at all orientations—i.e. its polarizability will be exactly the same in any direction across the axis. This means that a section through the polarizability ellipsoid will be circular, which is what we have drawn in Fig. 4.1(*c*).

If the field is applied *along* the bond axis, as in Fig. 4.1(*b*), the polarizability is greater, as we mentioned earlier. Thus the cross-section of the ellipsoid is *less*, as shown in Fig. 4.1(*d*).

The student must not make the mistake of confusing a polarizability ellipsoid with electron orbitals or electron clouds. In a sense the polarizability ellipsoid is the *inverse* of an electron cloud—where the electron cloud is largest the electrons are further from the nucleus and so are most easily polarized. This, as we have seen, is represented by a *small* axis for the polarizability ellipsoid.

All diatomic molecules have ellipsoids of the same general tangerine shape as H_2, as do linear polyatomic molecules, such as CO_2, $HC{\equiv}CH$, etc. They differ only in the relative sizes of their major and minor axes.

When a sample of such molecules is subjected to a beam of radiation of frequency ν the electric field experienced by each molecule varies according to the equation (cf. Eq. (1.1)):

$$E = E_0 \sin 2\pi\nu t \tag{4.2}$$

and thus the induced dipole also undergoes oscillations of frequency ν:

$$\mu = \alpha E = \alpha E_0 \sin 2\pi\nu t \tag{4.3}$$

Such an oscillating dipole emits radiation of its own oscillation frequency and we have immediately in Eq. (4.3) the classical explanation of Rayleigh scattering.

If, in addition, the molecule undergoes some internal motion, such as vibration or rotation, which *changes the polarizability* periodically, then the oscillating dipole will have superimposed upon it the vibrational or rotational oscillation. Consider, for example, a vibration of frequency $\nu_{\text{vib.}}$ which changes the polarizability: we can write

$$\alpha = \alpha_0 + \beta \sin 2\pi\nu_{\text{vib.}} t \tag{4.4}$$

where α_0 is the equilibrium polarizability and β represents the rate of change of polarizability with the vibration. Then we have:

$$\mu = \alpha E = (\alpha_0 + \beta \sin 2\pi \nu_{\text{vib.}} t) E_0 \sin 2\pi \nu t$$

or, expanding and using the trigonometric relation:

$$\sin A \sin B = \tfrac{1}{2}\{\cos(A - B) - \cos(A + B)\}$$

we have

$$\mu = \alpha_0 E_0 \sin 2\pi \nu t + \tfrac{1}{2}\beta E_0 \{\cos 2\pi(\nu - \nu_{\text{vib.}})t - \cos 2\pi(\upsilon + \nu_{\text{vib.}})t\} \qquad (4.5)$$

and thus the oscillating dipole has frequency components $\nu \pm \nu_{\text{vib.}}$ as well as the exciting frequency ν.

It should be carefully noted, however, that if the vibration does not alter the polarizability of the molecule (and we shall later give examples of such vibrations) then $\beta = 0$ and the dipole oscillates only at the frequency of the incident radiation; the same is true of a rotation. Thus we have the general rule:

> In order to be Raman active a molecular rotation or vibration must cause some change in a component of the molecular polarizability. A change in polarizability is, of course, reflected by a change in either the *magnitude* or the *direction* of the polarizability ellipsoid.

(This rule should be contrasted with that for infra-red and microwave activity, which is that the molecular motion must produce a change in the electric dipole of the molecule.)

Let us now consider briefly the shapes of the polarizability ellipsoids of more complicated molecules, taking first the bent triatomic molecule H_2O shown in Fig. 4.2(*a*). By analogy with the discussion for H_2 given above, we might expect the polarizability surface to be composed of *two* similar ellipsoids, one for each bond. While this may be correct in minute detail, we must remember that the oscillating electric field which we wish to apply for Raman spectroscopy is usually that of radiation in the visible or ultra-violet region, i.e. having a wavelength of some 1 μm–10 nm (cf. Fig. 1.4); molecular bonds, on the other hand, have dimensions of only some 0.1 nm, so we cannot expect our radiation to probe the finer details of bond polarizability—even the hardest of X-rays can scarcely do that. Instead the radiation can only sense the average polarizability in various directions through the molecule, and the polarizability ellipsoid, it may be shown, is always a true ellipsoid—i.e. a surface having *all* sections elliptical (or possibly circular). In the particular case of H_2O the polarizability is found to be different along all three of the major axes of the molecule (which lie along the line in the molecular plane bisecting the HOH angle, at right angles to this in the plane, and perpendicularly to the plane), and so all three of the ellipsoidal axes are also different; the ellipsoid is sketched in various orientations in Fig. 4.2(*b*). Other such molecules, for example H_2S or SO_2, have similarly shaped ellipsoids but with different dimensions.

Symmetric top molecules, because of their axial symmetry, have polarizability ellipsoids rather similar to those of linear molecules, i.e. with a circular cross-section at right angles to their axis of symmetry. It should be stressed, however, that sections in other planes are truly *elliptical*. For a molecule such as chloroform, $CHCl_3$ (Fig. 4.3(*a*)), where the chlorine atoms are bulky, the usual tendency is to draw the polarizability surface as egg-shaped, fatter at the chlorine-containing end. This is not correct; the polarizability ellipsoid for chloroform is shown at Fig. 4.3(*b*) where it will be seen that, since the polarizability is greater across the symmetry axis, the *minor* axis of the ellipsoid lies in this direction. Similar molecules are, for example, CH_3Cl and NH_3, etc. (although the latter fortuitously has a virtually spherical 'ellipsoid').

where α_0 is the equilibrium polarizability and β represents the rate of change of polarizability with the vibration. Then we have:

$$\mu = \alpha E = (\alpha_0 + \beta \sin 2\pi \nu_{\text{vib.}} t) E_0 \sin 2\pi \nu t$$

or, expanding and using the trigonometric relation:

$$\sin A \sin B = \tfrac{1}{2}\{\cos(A - B) - \cos(A + B)\}$$

we have

$$\mu = \alpha_0 E_0 \sin 2\pi \nu t + \tfrac{1}{2}\beta E_0 \{\cos 2\pi(\nu - \nu_{\text{vib.}})t - \cos 2\pi(\nu + \nu_{\text{vib.}})t\} \qquad (4.5)$$

and thus the oscillating dipole has frequency components $\nu \pm \nu_{\text{vib.}}$ as well as the exciting frequency ν.

It should be carefully noted, however, that if the vibration does not alter the polarizability of the molecule (and we shall later give examples of such vibrations) then $\beta = 0$ and the dipole oscillates only at the frequency of the incident radiation; the same is true of a rotation. Thus we have the general rule:

> In order to be Raman active a molecular rotation or vibration must cause some change in a component of the molecular polarizability. A change in polarizability is, of course, reflected by a change in either the *magnitude* or the *direction* of the polarizability ellipsoid.

(This rule should be contrasted with that for infra-red and microwave activity, which is that the molecular motion must produce a change in the electric dipole of the molecule.)

Let us now consider briefly the shapes of the polarizability ellipsoids of more complicated molecules, taking first the bent triatomic molecule H_2O shown in Fig. 4.2(*a*). By analogy with the discussion for H_2 given above, we might expect the polarizability surface to be composed of *two* similar ellipsoids, one for each bond. While this may be correct in minute detail, we must remember that the oscillating electric field which we wish to apply for Raman spectroscopy is usually that of radiation in the visible or ultra-violet region, i.e. having a wavelength of some 1 μm–10 nm (cf. Fig. 1.4); molecular bonds, on the other hand, have dimensions of only some 0.1 nm, so we cannot expect our radiation to probe the finer details of bond polarizability—even the hardest of X-rays can scarcely do that. Instead the radiation can only sense the average polarizability in various directions through the molecule, and the polarizability ellipsoid, it may be shown, is always a true ellipsoid—i.e. a surface having *all* sections elliptical (or possibly circular). In the particular case of H_2O the polarizability is found to be different along all three of the major axes of the molecule (which lie along the line in the molecular plane bisecting the HOH angle, at right angles to this in the plane, and perpendicularly to the plane), and so all three of the ellipsoidal axes are also different; the ellipsoid is sketched in various orientations in Fig. 4.2(*b*). Other such molecules, for example H_2S or SO_2, have similarly shaped ellipsoids but with different dimensions.

Symmetric top molecules, because of their axial symmetry, have polarizability ellipsoids rather similar to those of linear molecules, i.e. with a circular cross-section at right angles to their axis of symmetry. It should be stressed, however, that sections in other planes are truly *elliptical*. For a molecule such as chloroform, $CHCl_3$ (Fig. 4.3(*a*)), where the chlorine atoms are bulky, the usual tendency is to draw the polarizability surface as egg-shaped, fatter at the chlorine-containing end. This is not correct; the polarizability ellipsoid for chloroform is shown at Fig. 4.3(*b*) where it will be seen that, since the polarizability is greater across the symmetry axis, the *minor* axis of the ellipsoid lies in this direction. Similar molecules are, for example, CH_3Cl and NH_3, etc. (although the latter fortuitously has a virtually spherical 'ellipsoid').

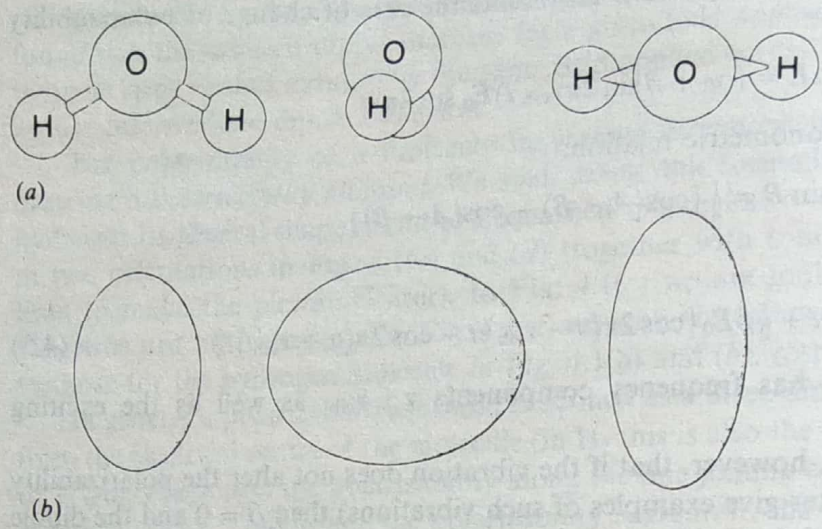

Figure 4.2 The water molecule and its polarizability ellipsoid, seen along the three main axes.

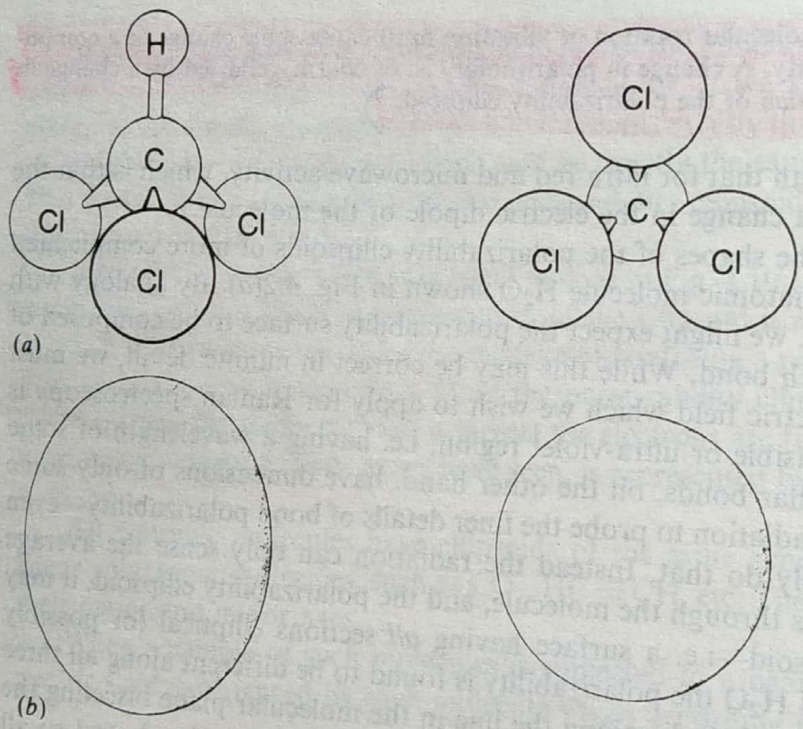

Figure 4.3 The chloroform molecule and its polarizability ellipsoid, seen from across and along the symmetry axis.

Finally, spherical top molecules, such as CH_4, CCl_4, SiH_4, etc., have spherical polarizability surfaces, since they are completely isotropic as far as incident radiation is concerned.

We are now in a position to discuss in detail the Raman spectra of various types of molecule. Since we shall be dealing with rotational and vibrational changes it is evident that expressions for the energy levels and for many of the allowed transitions will be identical with those already discussed in the previous two chapters. For clarity we shall repeat any such expressions but not rederive them, being content to give a cross-reference to where their derivation may be found.

4.2 PURE ROTATIONAL RAMAN SPECTRA

4.2.1 Linear Molecules

The rotational energy levels of linear molecules have already been stated (cf. Eq. (2.24)):

$$\varepsilon_J = BJ(J+1) - DJ^2(J+1)^2 \quad \text{cm}^{-1} \quad (J = 0, 1, 2, \ldots)$$

but, in Raman spectroscopy, the precision of the measurements does not normally warrant the retention of the term involving D, the centrifugal distortion constant. Thus we take the simpler expression:

$$\varepsilon_J = BJ(J+1) \quad \text{cm}^{-1} \quad (J = 0, 1, 2, \ldots) \tag{4.6}$$

to represent the energy levels.

Transitions between these levels follow the formal selection rule:

$$\Delta J = 0, \text{ or } \pm 2 \text{ only} \tag{4.7}$$

which is to be contrasted with the corresponding selection rule for microwave spectroscopy, $\Delta J = \pm 1$, given in Eq. (2.17). The fact that in Raman work the rotational quantum number changes by two units rather than one is connected with the symmetry of the polarizability ellipsoid. For a linear molecule, such as is depicted in Fig. 4.1, it is evident that during end-over-end rotation the ellipsoid presents the same appearance to an observer *twice* in every complete rotation. It is equally clear that rotation about the bond axis produces no change in polarizability and hence, as in infra-red and microwave spectroscopy, we need concern ourselves only with end-over-end rotations.

If, following the usual practice, we define ΔJ as $(J_{\text{upper state}} - J_{\text{lower state}})$ then we can ignore the selection rule $\Delta J = -2$ since, for a pure rotational change, the upper state quantum number must necessarily be greater than that in the lower state. Further, the 'transition' $\Delta J = 0$ is trivial since this represents no change in the molecular energy and hence Rayleigh scattering only.

Combining, then, $\Delta J = +2$ with the energy levels of Eq. (4.6) we have:

$$\begin{aligned} \Delta\varepsilon &= \varepsilon_{J'=J+2} - \varepsilon_{J''=J} \\ &= B(4J+6) \quad \text{cm}^{-1} \end{aligned} \tag{4.8}$$

Since $\Delta J = +2$, we may label these lines S branch lines (cf. Sec. 3.2) and write

$$\Delta\varepsilon_S = B(4J+6) \quad \text{cm}^{-1} \qquad (J = 0, 1, 2, \ldots) \tag{4.9}$$

where J is the rotational quantum number in the *lower* state.

Thus if the molecule gains rotational energy from the photon during collision we have a series of S branch lines to the low wavenumber side of the exciting line (Stokes' lines), while if the molecule loses energy to the photon the S branch lines appear on the high wavenumber side (anti-Stokes' lines). The wavenumbers of the corresponding spectral lines are given by:

$$\bar{\nu}_S = \bar{\nu}_{\text{ex.}} \pm \Delta\varepsilon_S = \bar{\nu}_{\text{ex.}} \pm B(4J+6) \quad \text{cm}^{-1} \tag{4.10}$$

where the plus sign refers to anti-Stokes' lines, the minus to Stokes' lines, and $\bar{\nu}_{\text{ex.}}$ is the wavenumber of the exciting radiation.

The allowed transitions and the Raman spectrum arising are shown schematically in Fig. 4.4. Each transition is labelled according to its lower J value and the relative intensities of the lines are indicated assuming that the population of the various energy levels varies according to Eq. (2.21) and Fig. 2.7. In particular it should be noted here that Stokes' and anti-Stokes' lines have comparable intensity because many rotational levels are populated and hence downward transitions are approximately as likely as upward ones.

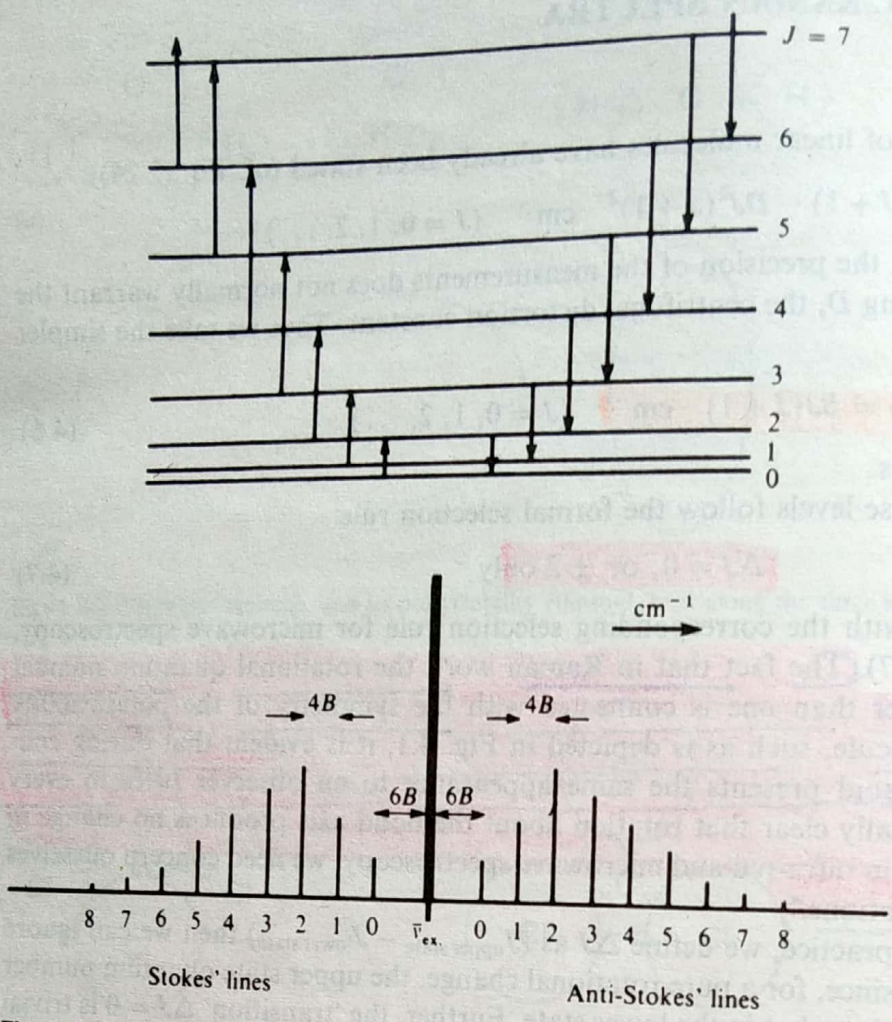

Figure 4.4 The rotational energy levels of a diatomic molecule and the rotational Raman spectrum arising from transitions between them. Spectral lines are numbered according to their lower J values.

When the value $J = 0$ is inserted into Eq. (4.10) it is seen immediately that the separation of the first line from the exciting line is $6B\,\text{cm}^{-1}$, while the separation between successive lines is $4B\,\text{cm}^{-1}$. For diatomic and light triatomic molecules the rotational Raman spectrum will normally be resolved and we can immediately obtain a value of B, and hence the moment of inertia and bond lengths for such molecules. If we recall that homonuclear diatomic molecules (for example O_2, H_2) give no infra-red or microwave spectra since they possess no dipole moment, whereas they *do* give a rotational Raman spectrum, we see that the Raman technique yields structural data unobtainable from the techniques previously discussed. It is thus complementary to microwave and infra-red studies, not merely confirmatory.

It should be mentioned that, if the molecule has a centre of symmetry (as, for example, do H_2, O_2, CO_2), then the effects of nuclear spin will be observed in the Raman as in the infra-red. Thus for O_2 and CO_2 (since the spin of oxygen is zero) every alternate rotational level is absent; for example, in the case of O_2, every level with *even* J values is missing, and thus every transition labelled $J = 0, 2, 4, \ldots$ in Fig. 4.4 is also completely missing from the spectrum. In the case of H_2, and other molecules composed of nuclei with non-zero spin, the spectral lines show an alternation of intensity.

Linear molecules with more than three heavy atoms have large moments of inertia and their rotational fine structure is often unresolved in the Raman spectrum. Direct structural information is not, therefore, obtainable, but we shall see shortly that, taken in conjunction with the infra-red spectrum, the Raman can still yield much very useful information.

4.2.2 Symmetric Top Molecules

The polarizability ellipsoid for a typical symmetric top molecule, for example $CHCl_3$, was shown in Fig. 4.3(*b*). Plainly rotation about the top axis produces no change in the polarizability, but end-over-end rotations will produce such a change.

From Eq. (2.38) we have the energy levels:

$$\varepsilon_{J,K} = BJ(J+1) + (A-B)K^2 \quad \text{cm}^{-1}$$
$$(J = 0, 1, 2, \ldots;\ K = \pm J, \pm(J-1), \ldots) \tag{4.11}$$

The selection rules for Raman spectra are:

$$\left.\begin{aligned} &\Delta K = 0 \\ &\Delta J = 0, \pm 1, \pm 2 \quad \text{(except for } K = 0 \text{ states} \\ &\qquad\qquad\qquad\qquad \text{when } \Delta J = \pm 2 \text{ only)} \end{aligned}\right\} \tag{4.12}$$

K, it will be remembered, is the rotational quantum number for axial rotation, so the selection rule $\Delta K = 0$ implies that changes in the angular momentum about the top axis will not give rise to a Raman spectrum—such rotations are, as mentioned previously, Raman inactive. The restriction of ΔJ to ± 2 for $K = 0$ states means effectively that ΔJ cannot be ± 1 for transitions involving the ground state ($J = 0$) since $K = \pm J, \pm(J-1), \ldots, 0$. Thus for all J values other than zero, K also may be different from zero and $\Delta J = \pm 1$ transitions are allowed.

Restricting ourselves, as before, to positive ΔJ we have the two cases:

1. $\Delta J = +1$ (R branch lines)

$$\begin{aligned} \Delta\varepsilon_R &= \varepsilon_{J'=J+1} - \varepsilon_{J''=J} \\ &= 2B(J+1) \quad \text{cm}^{-1} \qquad (J = 1, 2, 3, \ldots \quad (\text{but } J \neq 0)) \end{aligned} \tag{4.13a}$$

2. $\Delta J = +2$ (S branch lines)

$$\begin{aligned} \Delta\varepsilon_S &= \varepsilon_{J'=J+2} - \varepsilon_{J''=J} \\ &= B(4J+6) \quad \text{cm}^{-1} \qquad (J = 0, 1, 2, \ldots) \end{aligned} \tag{4.13b}$$

Thus we shall have two series of lines in the Raman spectrum:

$$\left.\begin{aligned} \bar{\nu}_R &= \bar{\nu}_{\text{ex.}} \pm \Delta\varepsilon_R = \bar{\nu}_{\text{ex.}} \pm 2B(J+1) \quad \text{cm}^{-1} \quad (J = 1, 2, \ldots) \\ \bar{\nu}_S &= \bar{\nu}_{\text{ex.}} \pm \Delta\varepsilon_S = \bar{\nu}_{\text{ex.}} \pm B(4J+6) \quad \text{cm}^{-1} \quad (J = 0, 1, 2, \ldots) \end{aligned}\right\} \tag{4.14}$$

These series are sketched separately in Fig. 4.5(*a*) and (*b*), where each line is labelled with its corresponding *lower* J value. In the R branch, lines appear at $4B$, $6B$, $8B$, $10B$, . . . cm^{-1} from the exciting line, while the S branch series occurs at $6B$, $10B$, $14B$, . . . cm^{-1}. The complete spectrum, shown in Fig. 4.5(*c*) illustrates how every alternate R line is overlapped by an S line. Thus a marked intensity alternation is to be expected which, it should be noted, is not connected with nuclear spin statistics.

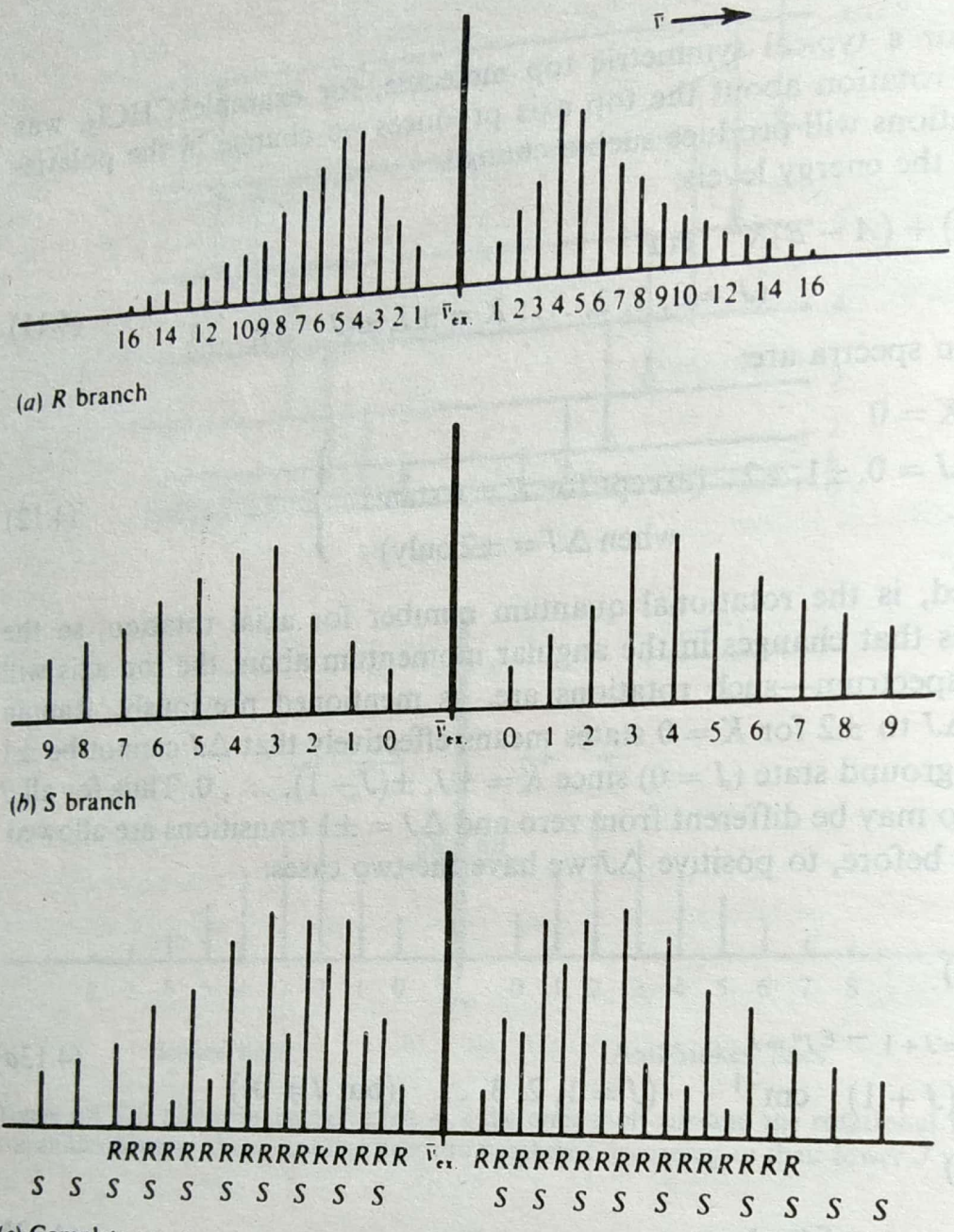

Figure 4.5 The rotational Raman spectrum of a symmetric top molecule. The *R* and *S* branch lines are shown separately in (*a*) and (*b*), respectively, with the total spectrum in (*c*).

Normally *all* rotations of asymmetric top molecules, on the other hand, are Raman active. Their Raman spectra are thus quite complicated and will not be dealt with in detail here; it suffices to say that, as in the microwave region, the spectra may often be interpreted by considering the molecule as intermediate between the oblate and prolate types of symmetric top.

4.3 VIBRATIONAL RAMAN SPECTRA

4.3.1 Raman Activity of Vibrations

If a molecule has little or no symmetry it is a very straightforward matter to decide whether its vibrational modes will be Raman active or inactive: in fact, it is usually correct to assume that *all* its modes are Raman active. However, when the molecule has considerable symmetry it is not always easy to make the decision, since it is sometimes not clear, without detailed consideration, whether or not the polarizability changes during the vibration.

We consider first the simple asymmetric top molecule H_2O whose polarizability ellipsoid was shown in Fig. 4.2. In Fig. 4.6 we illustrate in (*a*), (*b*), and (*c*), respectively, the three fundamental modes ν_1, ν_2, and ν_3, sketching for each mode the equilibrium configuration in the centre with the extreme positions to right and left. The approximate shapes of the corresponding polarizability ellipsoids are also shown.

During the symmetric stretch, in Fig. 4.6(*a*), the molecule as a whole increases and decreases in size; when a bond is stretched, the electrons forming it are less firmly held by the nuclei and so the bond becomes more polarizable. Thus the polarizability ellipsoid of H_2O may be expected to decrease in size while the bonds stretch, and to increase while they compress, but to maintain an

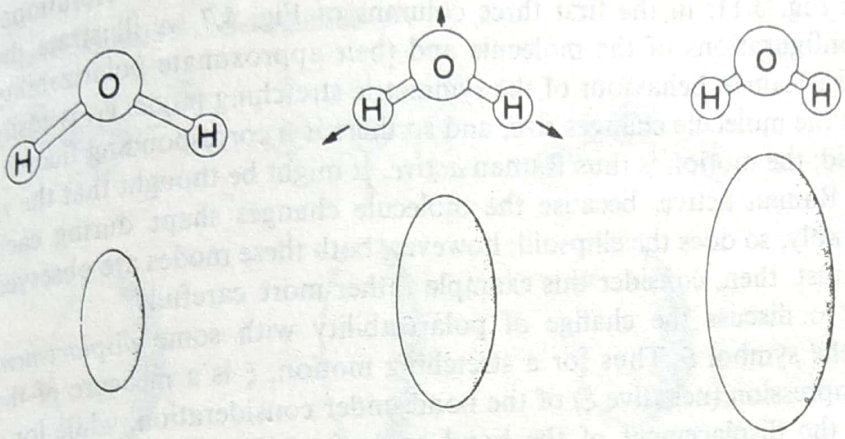

(*a*) ν_1, symmetric stretching mode

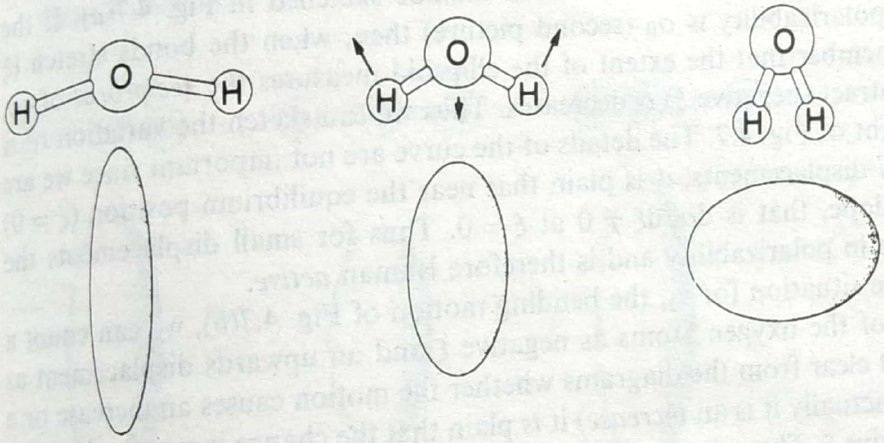

(*b*) ν_2, bending mode

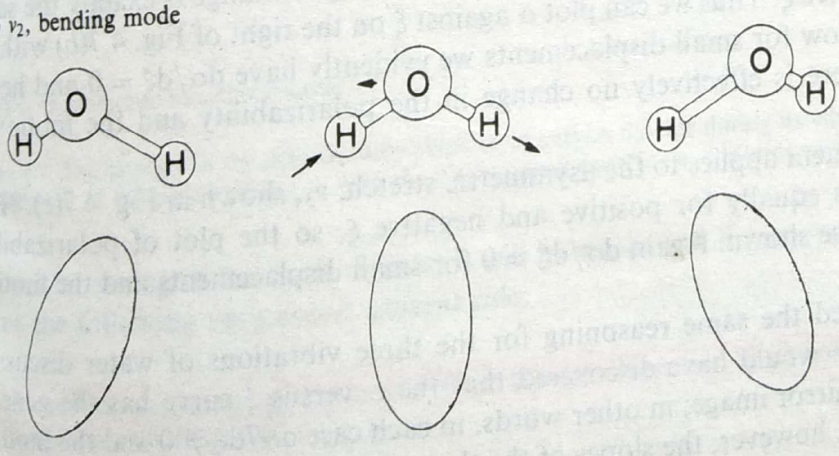

(*c*) ν_3, asymmetric stretching mode

Figure 4.6 The change in size, shape, or direction of the polarizability ellipsoid of the water molecule during each of its three vibrational modes. The centre column shows the equilibrium position of the molecule, while to right and left are the (exaggerated) extremes of each vibration.

approximately constant shape. On the other hand, while undergoing the bending motion, in Fig. 4.6(*b*), it is the shape of the ellipsoid which changes most; thus if we imagine vibrations of very large amplitude, at one extreme (on the left) the molecule approaches the linear configuration with a horizontal axis, while at the other extreme (on the right) it approximates to a diatomic molecule (if the two H atoms are almost coincidental) with a vertical axis. Finally in Fig. 4.6(*c*) we have the asymmetric stretching motion, ν_3, where both the size and shape remain approximately constant, but the direction of the major axis changes markedly. Thus all three vibrations involve obvious changes in at least one aspect of the polarizability ellipsoid, and all are Raman *active*.

Now consider the linear triatomic molecule CO_2, whose three fundamental vibrational modes have been shown in Fig. 3.11; in the first three columns of Fig. 4.7 we illustrate the extreme and equilibrium configurations of the molecule and their approximate polarizability ellipsoids. The question of the Raman behaviour of the symmetric stretching mode, ν_1, is easily decided—during the motion the molecule changes size, and so there is a corresponding fluctuation in the size of the ellipsoid; the motion is thus Raman *active*. It might be thought that the ν_2 and ν_3 vibrations are also Raman active, because the molecule changes shape during each vibration and hence, presumably, so does the ellipsoid; however, both these modes are observed to be Raman *inactive*. We must, then, consider this example rather more carefully.

To do this it is usual to discuss the change of polarizability with some *displacement coordinate*, normally given the symbol ξ. Thus for a stretching motion, ξ is a measure of the extension (positive ξ) or compression (negative ξ) of the bond under consideration, while for a bending mode, ξ measures the displacement of the bond angle from its equilibrium value, positive and negative ξ referring to opposite displacement directions.

Consider, as an example, the ν_1 stretch of carbon dioxide sketched in Fig. 4.7(*a*). If the equilibrium value of the polarizability is α_0 (second picture) then, when the bonds stretch (ξ positive), α increases (remember that the extent of the ellipsoid measures the *reciprocal* of α), while when the bonds contract (negative ξ) α decreases. Thus we can sketch the variation of α with ξ as shown on the right of Fig. 4.7. The details of the curve are not important since we are concerned only with *small* displacements; it is plain that near the equilibrium position ($\xi = 0$) the curve has a distinct slope, that is $d\alpha/d\xi \neq 0$ at $\xi = 0$. Thus for small displacements the motion produces a change in polarizability and is therefore Raman *active*.

If we now consider the situation for ν_2, the bending motion of Fig. 4.7(*b*), we can count a downwards displacement of the oxygen atoms as negative ξ and an upwards displacement as positive. Although it is not clear from the diagrams whether the motion causes an increase or a decrease in polarizability (actually it is an *increase*) it *is* plain that the change is exactly the same for both positive and negative ξ. Thus we can plot α against ξ on the right of Fig. 4.7(*b*) with, as before, $\alpha = \alpha_0$ at $\xi = 0$. Now for small displacements we evidently have $d\alpha/d\xi = 0$ and hence for *small displacements* there is effectively no change in the polarizability and the motion is Raman *inactive*.

Exactly the same argument applies to the asymmetric stretch, ν_3, shown in Fig. 4.7(*c*). Here the polarizability decreases equally for positive and negative ξ, so the plot of polarizability against ξ has the appearance shown. Again $d\alpha/d\xi = 0$ for small displacements and the motion is Raman *inactive*.

We could have followed the same reasoning for the three vibrations of water discussed previously. In each case we would have discovered that the α versus ξ curve has the general shape of Fig. 4.7(*a*) or its mirror image; in other words, in each case $d\alpha/d\xi \neq 0$ and the motion is Raman *active*. In general, however, the slopes of the three curves would be different at $\xi = 0$, that is $d\alpha/d\xi$ would have different values. Since we have seen that the Raman spectrum is forbidden for $d\alpha/d\xi = 0$ but allowed for $d\alpha/d\xi \neq 0$ we can imagine that the 'degree of allowedness' varies with $d\alpha/d\xi$. Thus if the polarizability curve has a large slope at $\xi = 0$ the Raman

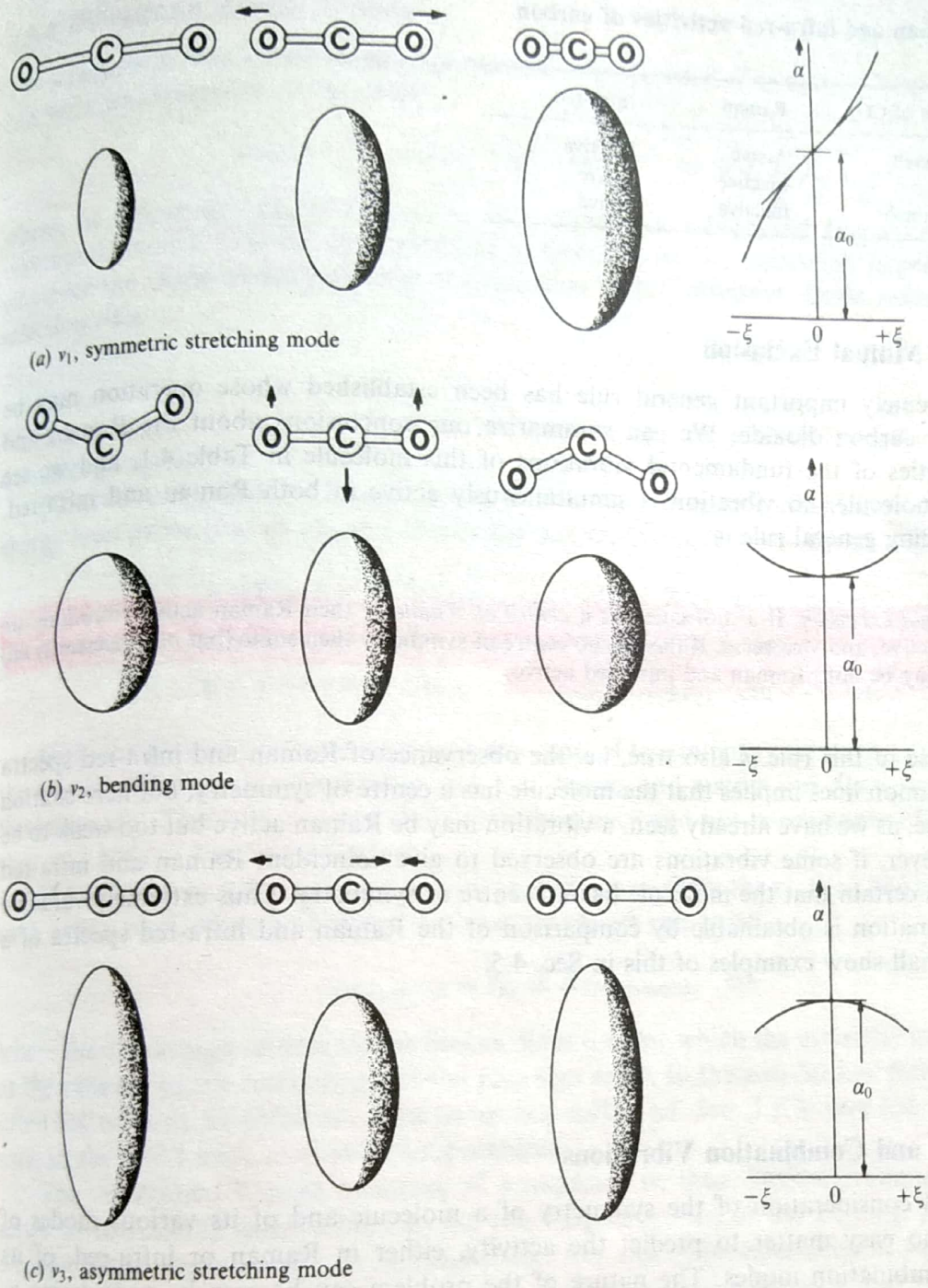

(a) ν_1, symmetric stretching mode

(b) ν_2, bending mode

(c) ν_3, asymmetric stretching mode

Figure 4.7 The changes in the polarizability ellipsoid of carbon dioxide during its vibrations, and a graph showing the variation of the polarizability, α, with the displacement coordinate, ξ, during each vibration.

line will be strong; if the slope is small it will be weak; and if zero, not allowed at all. From this stems the following very useful general rule:

Symmetric vibrations give rise to intense Raman lines; non-symmetric ones are usually weak and sometimes unobservable.

In particular, a bending motion usually yields only a very weak Raman line; e.g. the ν_2 motion of H_2O (Fig. 4.6(*b*)), although allowed in the Raman, has not been observed, nor has ν_3, for which $d\alpha/d\xi$ is also small.

Table 4.1 Raman and infra-red activities of carbon dioxide

Mode of vibration of CO_2	Raman	Infra-red
ν_1 : symmetric stretch	Active	Inactive
ν_2 : bend	Inactive	Active
ν_3 : asymmetric stretch	Inactive	Active

4.3.2 Rule of Mutual Exclusion

A further extremely important general rule has been established whose operation may be exemplified by carbon dioxide. We can summarize our conclusions about the Raman and infra-red activities of the fundamental vibrations of this molecule in Table 4.1, and we see that, for this molecule, no vibration is simultaneously active in both Raman and infra-red. The corresponding general rule is:

Rule of mutual exclusion. If a molecule has a *centre of symmetry* then Raman active vibrations are infra-red inactive, and vice versa. If there is no centre of symmetry then some (but not necessarily all) vibrations may be both Raman and infra-red active.

The converse of this rule is also true, i.e. the observance of Raman and infra-red spectra showing no common lines implies that the molecule has a centre of symmetry; but here caution is necessary since, as we have already seen, a vibration may be Raman active but too weak to be observed. However, if some vibrations are observed to give coincident Raman and infra-red absorptions it is certain that the molecule has no centre of symmetry. Thus extremely valuable structural information is obtainable by comparison of the Raman and infra-red spectra of a substance; we shall show examples of this in Sec. 4.5.

4.3.3 Overtone and Combination Vibrations

Without detailed consideration of the symmetry of a molecule and of its various modes of vibration, it is no easy matter to predict the activity, either in Raman or infra-red, of its overtone and combination modes. The nature of the problem can be seen by considering ν_1 and ν_2 of carbon dioxide; the former is Raman active only, the latter infra-red active. What, then, of the activity of $\nu_1 + \nu_2$? In fact it is only infra-red active, but this is not at all obvious merely from considering the dipole or polarizability changes during the motions. Again, when discussing Fermi resonance (Sec. 3.5.2) we chose as an example the resonance of ν_1 and $2\nu_2$ of carbon dioxide in the *Raman* effect. Thus $2\nu_2$ is Raman active although the fundamental ν_2 is only infra-red active.

We shall not attempt here to discuss this matter further, being content to leave the reader with a warning that the activity or inactivity of a fundamental in a particular type of spectroscopy does not necessarily imply corresponding behaviour of its overtones or combinations, particularly if the molecule has considerable symmetry. A more detailed discussion is to be found in Herzberg's book *Infra-red and Raman Spectra* and others mentioned in the bibliography.

4.3.4 Vibrational Raman Spectra

The structure of vibrational Raman spectra is easily discussed. For every vibrational mode we can write an expression of the form:

$$\varepsilon = \bar{\omega}_e(v + \tfrac{1}{2}) - \bar{\omega}_e x_e(v + \tfrac{1}{2})^2 \quad \text{cm}^{-1} \qquad (v = 0, 1, 2, \ldots) \tag{4.15}$$

where, as before (cf. Eq. (3.12)), $\bar{\omega}_e$ is the equilibrium vibrational frequency expressed in wavenumbers and x_e is the anharmonicity constant. Such an expression is perfectly general, whatever the shape of the molecule or the nature of the vibration. Quite general, too, is the selection rule:

$$\Delta v = 0, \pm 1, \pm 2, \ldots \tag{4.16}$$

which is the same for Raman as for infra-red spectroscopy, the probability of $\Delta v = \pm 2, \pm 3, \ldots$ decreasing rapidly.

Particularizing, now, to Raman active modes, we can apply the selection rule (4.16) to the energy level expression (4.15) and obtain the transition energies (cf. Eq. (3.15)):

$$\left.\begin{aligned} v = 0 \rightarrow v = 1\text{: } \Delta\varepsilon_{\text{fundamental}} &= \bar{\omega}_e(1 - 2x_e) \quad \text{cm}^{-1} \\ v = 0 \rightarrow v = 2\text{: } \Delta\varepsilon_{\text{overtone}} &= 2\bar{\omega}_e(1 - 3x_e) \quad \text{cm}^{-1} \\ v = 1 \rightarrow v = 2\text{: } \Delta\varepsilon_{\text{hot}} &= \bar{\omega}_e(1 - 4x_e) \quad \text{cm}^{-1} \qquad \text{etc.} \end{aligned}\right\} \tag{4.17}$$

Since the Raman scattered light is, in any case, of low intensity we can ignore completely all the weaker effects such as overtones and 'hot' bands, and restrict our discussion merely to the fundamentals. This is not to say that active overtones and hot bands cannot be observed, but they add little to the discussion here.

We would expect Raman lines to appear at distances from the exciting line corresponding to each active fundamental vibration. In other words we can write:

$$\bar{\nu}_{\text{fundamental}} = \bar{\nu}_{\text{ex.}} \pm \Delta\varepsilon_{\text{fundamental}} \quad \text{cm}^{-1} \tag{4.18}$$

where the minus sign represents the Stokes' lines (i.e. for which the molecule has gained energy at the expense of the radiation) and the plus sign refers to the anti-Stokes' lines. The latter are often too weak to be observed, since as we saw earlier (cf. Sec. 3.1.3) very few of the molecules exist in the $v = 1$ state at normal temperatures.

The vibrational Raman spectrum of a molecule is, then, basically simple. It will show a series of reasonably intense lines to the low-frequency side of the exciting line with a much weaker, mirror-image series on the high-frequency side. The separation of each line from the centre of the exciting line gives immediately the Raman active fundamental vibration frequencies of the molecule.

As an example we illustrate the Raman spectrum of chloroform, $CHCl_3$, a symmetric top molecule (Fig. 4.8(*a*)). The exciting line in this case is the 488 nm argon ion laser line (at a power of 100 mW), and a wavenumber scale is drawn from this line as zero. Raman lines appear at 262, 366, 668, 761, 1216, and 3019 cm^{-1} on the low-frequency (Stokes') side of the exciting line while the line at 262 cm^{-1} on the frequency (anti-Stokes') side is included for a comparison of its intensity.

For comparison also we show at Fig. 4.8(*b*) the *infra-red* spectrum of the same molecule. The range of the instrument used precluded measurements below 600 cm^{-1}, but we see clearly that strong (and hence fundamental) lines appear in the spectrum at wavenumbers corresponding very precisely with those of lines in the Raman spectrum but with very different relative intensities.

CHAPTER SEVEN

SPIN RESONANCE SPECTROSCOPY

We have seen in earlier chapters that all electrons and some nuclei possess a property conveniently called 'spin'. Electronic spin was introduced in Chapter 5 to account for the way in which electrons group themselves about a nucleus to form atoms and we found that the spin also accounted for some fine structure, such as the doublet nature of the sodium D line, in atomic spectra. Equally, in Sec. 5.6 it was necessary to invoke a nuclear spin to account for very tiny effects, called hyperfine structure, observed in the spectra of some atoms.

In this chapter we shall consider these spins in rather more detail and discuss the sort of spectra they can give rise to directly rather than their influence on other types of spectra. After an introduction discussing the interaction of spin with an external magnetic field we shall consider in some detail the spectra of particles with a spin of $\frac{1}{2}$ (i.e. electrons and some nuclei such as hydrogen, fluorine, or phosphorus), then a brief discussion of some other nuclei whose spins are greater than $\frac{1}{2}$, and finally a few words on the techniques involved in producing electronic and nuclear spin spectra.

7.1 SPIN AND AN APPLIED FIELD

7.1.1 The Nature of Spinning Particles

We have seen that all electrons have a spin of $\frac{1}{2}$, that is they have an angular momentum of $\sqrt{[\frac{1}{2}(\frac{1}{2}+1)]}(h/2\pi) = \sqrt{3/2}$ units. Many nuclei also possess spin although the angular momentum concerned varies from nucleus to nucleus.

The simplest nucleus is that of the hydrogen atom, which consists of one particle only, the *proton*. The protonic mass (1.67×10^{-27} kg) and charge ($+1.60 \times 10^{-19}$ C) are taken as the units of atomic mass and charge, respectively; the charge is, of course, equal in magnitude but opposite in sign to the electronic charge. The proton also has a spin of $\frac{1}{2}$.

Another particle which is a constituent of all nuclei (apart from the hydrogen nucleus) is the *neutron*; this has unit mass (i.e. a mass equal to that of the proton), no charge, and, again, a spin of $\frac{1}{2}$.

Thus if a particular nucleus is composed of p protons and n neutrons its total mass is $p+n$ (ignoring the small mass defects associated with nuclear binding energy), its total charge is $+p$, and its total spin will be a vector combination of $p+n$ spins each of magnitude $\frac{1}{2}$. The atomic mass is usually specified for each nucleus by writing it as a prefix to the nuclear symbol; for example ^{12}C indicates the nucleus of carbon having a mass of 12. Since the atomic charge is six for this nucleus we know immediately that the nucleus must contain six protons and six neutrons to make up a mass of 12. The nucleus ^{13}C (an *isotope* of carbon) has six protons and seven neutrons.

Each nuclear isotope, being composed of a different number of protons and neutrons, will have its own total spin value. Unfortunately, the laws governing the vector addition of nuclear spins are not yet known so the spin of a particular nucleus cannot be predicted in general. However, observed spins can be rationalized and some empirical rules have been formulated.

Thus the spin of the hydrogen nucleus (^1H) is $\frac{1}{2}$ since it consists of one proton only; deuterium, an isotope of hydrogen containing one proton and one neutron (that is ^2H) might have a spin of 1 or 0 depending on whether the proton and neutron spins are parallel or opposed: it is observed to be 1. The helium nucleus, containing two protons and two neutrons (^4He), has zero spin, and from these and other observations stem the following rules:

1. Nuclei with both p and n even (hence charge *and* mass even) have zero spin (for example ^4He, ^{12}C, ^{16}O, etc.).
2. Nuclei with both p and n odd (hence charge *odd* but mass $= p+n$, *even*) have integral spin (for example ^2H, ^{14}N (spin $= 1$), ^{10}B (spin $= 3$), etc.).
3. Nuclei with odd mass have half-integral spins (for example ^1H, ^{15}N (spin $= \frac{1}{2}$), ^{17}O (spin $= \frac{5}{2}$), etc.).

The spin of a nucleus is usually given the symbol I, called the *spin quantum number*. Quantum mechanics shows that the angular momentum of a nucleus is given by the expression:

$$\text{Angular momentum } \mathbf{I} = \sqrt{I(I+1)}(h/2\pi) = \sqrt{I(I+1)} \text{ units} \tag{7.1}$$

where I takes, for each nucleus, *one* of the values, $0, \frac{1}{2}, 1, \frac{3}{2}, \ldots$. We can conveniently include the spin quantum number and angular momentum of an *electron* in Eq. (7.1) if we agree to label its spin quantum number I (instead of s as in Chapter 5), and remember that I can be $\frac{1}{2}$ only for an electron. Thus Eq. (7.1) represents the angular momentum of nuclei and of electrons once the appropriate value of I is inserted.

We may note here that many texts use a simpler form of Eq. (7.1), viz.:

$$\mathbf{I} = I\,\frac{h}{2\pi} = I \text{ units}$$

This equation is not, however, strictly correct from a quantum mechanical point of view and we shall use the more rigorous equation (7.1) throughout this chapter.

By now the reader will be familiar with the idea that the angular momentum vector $\mathbf{I}$ cannot point in any arbitrary direction, but can point only so that its components along a particular reference direction are either all integral (if I is integral) or all half-integral (if I is half-integral). Thus we can have components along a particular direction z, of:

$$I_z = I,\ I-1,\ \ldots,\ 0,\ \ldots,\ -(I-1),\ -I \quad \text{(for } I \text{ integral)}$$
$$I_z = I,\ I-1,\ \ldots,\ \tfrac{1}{2},\ -\tfrac{1}{2},\ \ldots,\ -I \quad \text{(for } I \text{ half-integral)} \qquad (7.2)$$

or

giving $2I+1$ components in each case. These components are normally degenerate—i.e. they all have the same energy—but the degeneracy may be lifted and $2I+1$ different energy levels result if an external magnetic field is applied to define the reference direction. We shall now consider the effect of such a field.

7.1.2 Interaction between Spin and a Magnetic Field

In general, a charged particle spinning about an axis constitutes a circular electric current which in turn produces a magnetic dipole. In other words the spinning particle behaves as a tiny bar magnet placed along the spin axis. The size of the dipole (i.e. the strength of the magnet) for a point charge can be shown to be:

$$\boldsymbol{\mu} = \frac{q}{2m}\mathbf{I} = \frac{q\sqrt{I(I+1)}}{2m}\,\frac{h}{2\pi} = \frac{qh}{4\pi m}\sqrt{I(I+1)} \quad \mathrm{A\,m^2}$$

where q and m are the charge and mass of the particle. The magnetic moment is here expressed in the appropriate fundamental SI units, ampere square metre ($\mathrm{A\,m^2}$); it is useful for later arguments, however, to express the magnetic moment in terms of the magnetic flux density (colloquially 'magnetic field strength'), the SI unit of which is the tesla (symbol T, units $\mathrm{kg\,s^{-2}\,A^{-1}}$), where $1\,\mathrm{T} \equiv 10\,000$ gauss. The conversion is:

$$\mathrm{A\,m^2} \equiv (\mathrm{kg\,s^{-2}\,T^{-1}})\,\mathrm{m^2} \equiv \mathrm{J\,T^{-1}} \text{ (joules per tesla)}$$

So we may write:

$$\mu = \frac{qh}{4\pi m}\sqrt{I(I+1)} \quad \mathrm{J\,T^{-1}} \qquad (7.3)$$

and it is this form we shall use in our subsequent discussion. (It should be pointed out that, when the magnetic moment is expressed in c.g.s. units, as in older textbooks, the right-hand side of Eq. (7.3) will be divided by c, the velocity of light.)

When we remove the fiction that electrons and nuclei are *point* charges, Eq. (7.3) becomes modified by the inclusion of a numerical factor G:

$$\mu = \frac{Gqh}{4\pi m}\sqrt{I(I+1)} \quad \mathrm{J\,T^{-1}} \qquad (7.4)$$

For electrons, we have seen (cf. Sec. 5.6) that G is given the symbol g and called the Landé splitting factor; its value depends on the quantum state of the electron and may be calculated from the L, S, and J quantum numbers (cf. Eq. (5.28)). Nuclear G factors, on the other hand, cannot be calculated in advance and are obtainable only experimentally.

For electrons, Eq. (7.4) is usually written:

$$\mu = -g\beta\sqrt{I(I+1)} \quad \mathrm{J\,T^{-1}} \qquad (7.5)$$

where we have expressed the set of constants $qh/4\pi m$ as a (positive) constant β, called the *Bohr magneton*, replacing the electronic charge (1.60×10^{-19} C) and mass (9.11×10^{-31} kg) in this expression, we can calculate $\beta = 9.273 \times 10^{-24}\,\mathrm{J\,T^{-1}}$.

Nuclear dipoles, on the other hand, are conveniently expressed in terms of a *nuclear magneton* β_N, which is defined in terms of the mass and charge of the *proton*:

$$\beta_N = \frac{eh}{4m_p\pi} = 5.050 \times 10^{-27}\ \mathrm{J\,T^{-1}}$$

Thus for a nucleus of mass M and charge pe (where p is the number of protons) we would write:

$$\mu = \frac{Gpe}{2M}\sqrt{I(I+1)}\ \frac{h}{2\pi} = \frac{Gm_p p}{M}\ \beta_N\sqrt{I(I+1)}$$
$$= g\beta_N\sqrt{I(I+1)}\ \ \mathrm{J\,T^{-1}} \qquad (7.6)$$

where we have collected the parameters $Gm_p p/M$, in which m_p is the protonic mass, into a factor g which is characteristic of each nucleus. This factor has values up to about six and is positive for nearly all known nuclei (see Table 7.1 later).

Thus the analogous equations (7.5) and (7.6) define the equivalent spin dipole for any spinning particle. The dipole will plainly have components along a reference direction governed by the I_z values:

$$\left.\begin{aligned} \mu_z &= -g\beta I_z \quad \text{(for electrons)} \\ \mu_z &= g\beta_N I_z \quad \text{(for nuclei)} \end{aligned}\right\} \qquad (7.7)$$

where the I_z are given by Eq. (7.2) for a particular particle, and the dipole will interact to different extents, depending on its magnitude, with a magnetic field. The situation for a *nucleus* with $I = 1$ is shown in Fig. 7.1. The angular momentum of the particle (Eq. (7.1)) is:

$$\mathbf{I} = \sqrt{1 \times 2} = \sqrt{2}\ \text{units}$$

and if we consider a semicircle with this radius, it is plain that the vector arrow corresponding to I can point so as to have z components of $+1$, 0, or -1 (the z direction is counted positive towards the top of the paper). This is shown in Fig. 7.1(a).

Equation (7.7) shows that μ_z and I_z have the same sign (i.e. point in the same direction) for the many nuclei which have positive g values. The three μ_z values for this system are represented by arrows in Fig. 7.1(b) where, conventionally, the lines of force inside the magnet are drawn

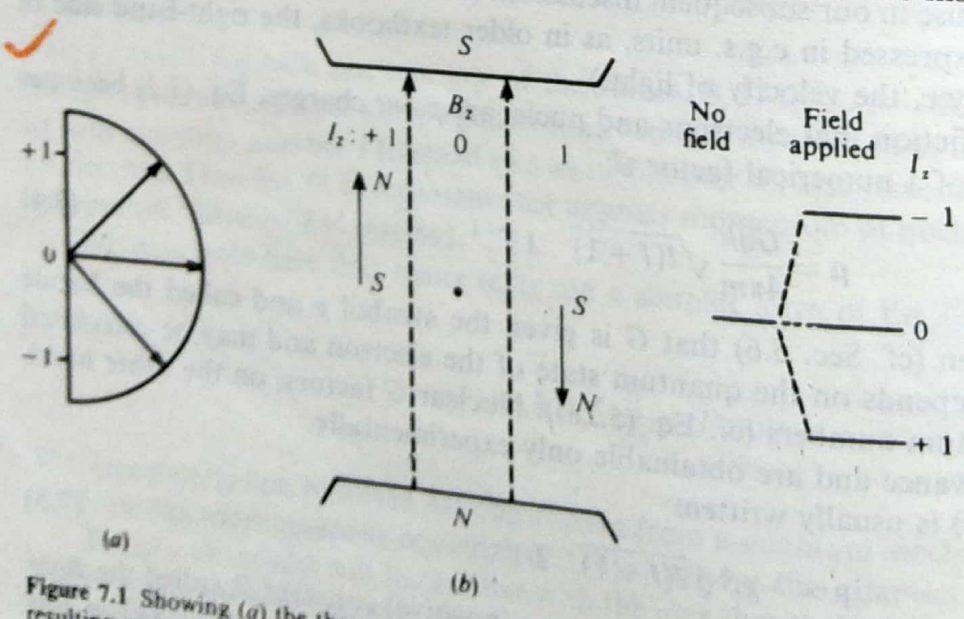

Figure 7.1 Showing (a) the three orientations of the spin of a nucleus with spin quantum number $I = 1$; (b) the resulting magnetic dipole, μ_z, oriented in an applied magnetic field B_z; and (c) the three energy levels allowed to the nucleus.

with an arrow pointing to the N pole. If we imagine the applied magnetic field to be produced by a horseshoe magnet and apply the same convention, it is clear that the lines of force *external* to the magnet will be shown pointing from the N to the S pole and, if we require these to be in the positive z direction, we arrive at the configuration given in Fig. 7.1(b). Thus we see that the state $I_z = -1$ represent a nuclear dipole *opposed* to the magnetic field (i.e. of high energy) while $I_z = +1$ is in the same direction as the applied field and is, therefore, of low energy. The state $I_z = 0$ has no net dipole along the field direction and is therefore unchanged in energy whether the field is applied or not. This is shown in Fig. 7.1(c).

Of course, if the nuclear g factor is negative, μ_z has a sign opposite from I_z, and the order of labelling the energy levels of Fig. 7.1 will be reversed. Similarly, of the two energy levels allowed to an electron in a magnetic field, the lower will be associated with $I_z = -\frac{1}{2}$, the upper with $I_z = +\frac{1}{2}$.

The extent of interaction between a magnetic dipole and a field of strength B_z applied along the z axis is equal to the product of the two:

$$\text{Interaction} = \mu_z B_z$$

Thus the separation between neighbouring energy levels (where I_z differs by unity) is:

$$\begin{aligned}\Delta E = |E_{I_z} - E_{(I_z-1)}| &= |g\beta_N I_z B_z - g\beta_N (I_z - 1)B_z| \\ &= |g\beta_N B_z| \quad \text{J} \qquad \text{(when } B_z \text{ is expressed in tesla)}\end{aligned} \tag{7.8}$$

Thus in hertz:

$$\frac{\Delta E}{h} = \left|\frac{g\beta_N B_z}{h}\right| \quad \text{Hz} \tag{7.9}$$

(where the modulus sign, $|\ldots|$, indicates that *positive* differences only should be considered). Here, then, is the basis for a spectroscopic technique: a transition of electron or nuclear spins between energy levels (loosely referred to as 'a change of spin') may be associated with the emission or absorption of energy in the form of radiation at the frequency of Eq. (7.9). Further, since the frequency is proportional to the applied field we can arrange, in principle, to study spin spectra in any region of the electromagnetic spectrum, merely by choosing an appropriate field. However, for practical reasons, the fields used are normally of the order of 1–5 tesla for nuclei and 0.3 tesla for electrons. Let us calculate the approximate frequency to be expected under these circumstances.

For nuclei: We have already $\beta_N = 5.05 \times 10^{-27}\ \text{J T}^{-1}$, and if we choose the rather specific value of $B_z = 2.3487\ \text{T}$ and the g factor of hydrogen, $g = 5.585$, we calculate:

$$\frac{\Delta E}{h} = \frac{5.585 \times 5.05 \times 10^{-27} \times 2.3487}{6.63 \times 10^{-34}} = 100 \times 10^6\ \text{Hz} \tag{7.10}$$

and we see that the appropriate frequency for protons, 100 MHz, falls in the short-wave radio-frequency region; in fact a great many nuclear magnetic resonance spectrometers operate at just this frequency, which is why we chose such a precise value of B_z for the calculation. All other nuclei (except tritium) have smaller g factors, and their spectra fall between 1 and 100 MHz for the same applied field. Table 7.1 collects some data for a few of the more important nuclei.

For electrons: Here $\beta = 9.273 \times 10^{-24}\ \text{J T}^{-1}$, and let us assume $g = 2$ and $B_z = 0.34\ \text{T}$. Then:

$$\frac{\Delta E}{h} = \frac{2 \times 9.273 \times 10^{-24} \times 0.34}{6.63 \times 10^{-34}} \approx 9500 \times 10^6\ \text{Hz} \tag{7.11}$$

Thus electron spin spectra fall at a considerably higher frequency, which is on the long wave-length edge of the microwave region. Because of this difference, techniques of nuclear and

Table 7.1 Properties of some nuclei with non-zero spin

Nucleus	Spin	Resonance frequency (MHz) in field of 2.3487 T	g value
^{1}H	$\frac{1}{2}$	100.00	5.585
^{10}B	3	10.75	0.6002
^{11}B	$\frac{3}{2}$	32.08	1.792
^{13}C	$\frac{1}{2}$	25.14	1.404
^{14}N	1	7.22	0.4036
^{15}N	$\frac{1}{2}$	10.13	−0.5660
^{17}O	$\frac{5}{2}$	13.56	−0.7572
^{19}F	$\frac{1}{2}$	94.07	5.255
^{29}Si	$\frac{1}{2}$	19.87	−1.110
^{31}P	$\frac{1}{2}$	40.48	2.261
^{35}Cl	$\frac{3}{2}$	9.80	0.5472
^{37}Cl	$\frac{3}{2}$	8.16	0.4555
^{107}Ag	$\frac{1}{2}$	4.05	−0.2260
^{119}Sn	$\frac{1}{2}$	37.27	−2.082
^{127}I	$\frac{5}{2}$	20.00	1.118
^{199}Hg	$\frac{1}{2}$	17.83	0.996

electronic spin spectroscopy differ considerably, as we shall see later, although in principle they are concerned with very similar phenomena.

Perhaps we should note that practitioners of nuclear magnetic resonance (n.m.r.) spectroscopy normally refer to the applied magnetic field as B_0 rather than the B_z which we have used above. For the remainder of Sec. 7.1, however, it is convenient to retain B_z (and later to introduce B_x and B_y) in order to emphasize the interaction of the spin vectors I_z with these fields. We will use B_0 for B_z (and B_1 for B_x) from Sec. 7.2 onwards.

7.1.3 Population of Energy Levels

When first confronted with nuclear and electron spin spectroscopy the student (who has experimented earlier with bar magnetics in the earth's field) usually asks: why don't the nuclear (or electronic) magnetic moments immediately line themselves up in an applied field so that they all occupy the lowest energy state?

There are several facets to this question and its answer. Firstly, if we take 'immediately' to refer to a period of some seconds, then spin magnetic moments *do* immediately orientate themselves in a magnetic field, although they do *not* all occupy the lowest available energy state. This is a simple consequence of thermal motion and the Boltzmann distribution. We have seen that spin energy levels are split in an applied field, and their energy separation (Eq. (7.8)) is ΔE joules. Let us confine our attention to particles with spin $\frac{1}{2}$ (and hence just two energy levels) for simplicity—our remarks, however, are easily extended to cover the general case. Classical theory states that at a temperature T K the ratio of the populations of such levels will be given by:

$$\frac{N_{\text{upper}}}{N_{\text{lower}}} = \exp\left(-\frac{\Delta E}{kT}\right) \tag{7.12}$$

where k is the Boltzmann constant. Thus at all temperatures above absolute zero the upper level will always be populated to some extent, although for large ΔE the population may be insignificant. In the case of nuclear and electron spins, however, ΔE is extremely small:

$$\Delta E \text{ nuclei} \quad \approx 7 \times 10^{-26} \text{ J} \quad \text{in a 2.3487 T field}$$

$$\Delta E \text{ electrons} \approx 6 \times 10^{-24} \text{ J} \quad \text{in a 0.34 T field}$$

and since $k = 1.38 \times 10^{-23} \text{ J K}^{-1}$, we have at room temperature ($T = 300$ K):

$$\frac{N_{\text{upper}}}{N_{\text{lower}}} \approx \exp\left(-\frac{7 \times 10^{-26}}{4.2 \times 10^{-21}}\right) \approx \exp(-1 \times 10^{-5})$$

$$\approx 1 - (1 \times 10^{-5}) \quad \text{for nuclei}$$

and

$$\frac{N_{\text{upper}}}{N_{\text{lower}}} \approx \exp\left(-\frac{6 \times 10^{-24}}{4.2 \times 10^{-21}}\right) \approx \exp(-1 \times 10^{-3})$$

$$\approx 1 - (1 \times 10^{-3}) \quad \text{for electrons}$$

In both cases the ratio is very nearly equal to unity and we see that the spins are almost equally distributed between the two (or, in general, $2I + 1$) energy levels.

We need to discuss now the nature of the interaction between radiation and the particle spins which can give rise to transitions between these levels.

7.1.4 The Larmor Precession

We have seen (Eq. (7.6)) that the dipole moment of a spinning nucleus is

$$\mu = g\beta_N \sqrt{I(I+1)} \quad \text{J T}^{-1}$$

and that, according to quantal laws, the vector represented by μ can be oriented only so that its components are integral or half-integral in a reference direction. The corollary to this is that, since $\sqrt{I(I+1)}$ cannot be integral or half-integral if I is integral or half-integral, the vector arrow can *never* be exactly in the field direction. We see one example of this in Fig. 7.1(a) and another for a nucleus with spin $\frac{1}{2}$ in Fig. 7.2(a). For such a particle:

$$\mu = g\beta_N \sqrt{3/2} \quad \text{and} \quad \mu_z = \pm \tfrac{1}{2} g\beta_N \quad \text{only}$$

Thus, whichever energy state a spinning nucleus or electron is in, it will always lie more or less across the field and will therefore be under the influence of a couple tending to turn it into the field direction.

Now the behaviour of a spinning nucleus or electron can be considered analogous to that of a gyroscope running in friction-free bearings. Experiments convince us that the application of a couple to a gyroscope does not cause its axis to tilt but merely induces a *precession* of the axis about the direction of the couple. Essentially the same occurs with a spinning particle and the precession, known as the Larmor precession, is sketched in Fig. 7.2(b). The precessional frequency (or Larmor frequency) is given by:

$$\omega = \frac{\text{magnetic moment}}{\text{angular momentum}} \times B_z \quad \text{rad s}^{-1}$$

$$= \frac{\mu B_z}{2\pi \mathbf{I}} \quad \text{Hz}$$

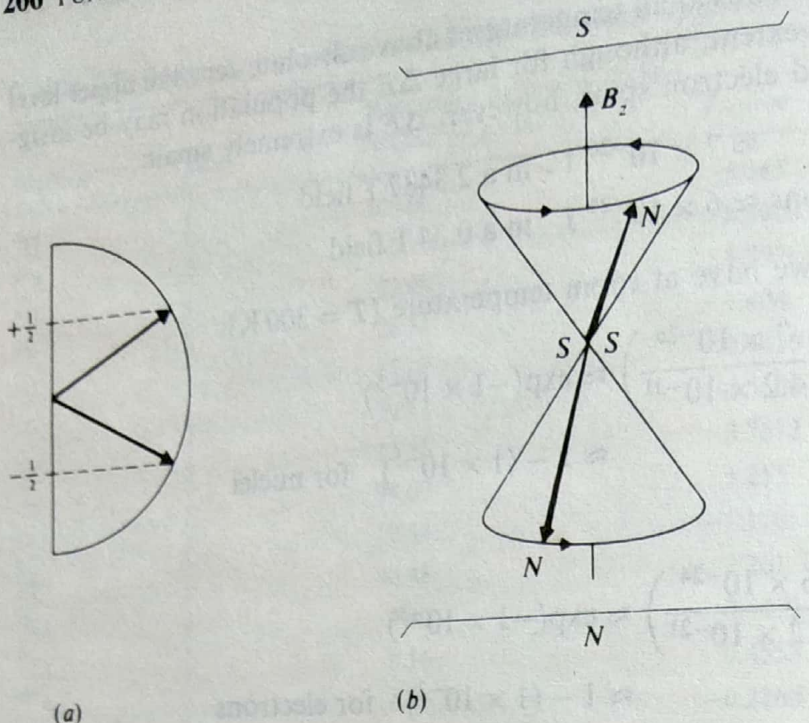

Figure 7.2 (*a*) The two spin orientations allowed to a nucleus with $I = \frac{1}{2}$ and (*b*) the Larmor precession of such a nucleus.

Replacing $\boldsymbol{\mu}$ and $\mathbf{I}$ by their expressions in Eqs (7.6) and (7.1):

$$\omega = \frac{g\beta_N\sqrt{I(I+1)}}{\sqrt{I(I+1)}\,(h/2\pi)}\,\frac{B_z}{2\pi} = \frac{g\beta_N B_z}{h} \quad \text{Hz}$$

and, comparing with Eq. (7.9), we see that the Larmor precessional frequency is just the frequency separation between energy levels.

This, then, is a mechanism by which particle spins can interact with a beam of electromagnetic radiation. If the beam has the same frequency as that of the precessing particle, it can interact coherently with the particle and energy can be exchanged; if it is of any other frequency, there will be no interaction. The phenomenon, then, is one of *resonance*. For nuclei it is referred to as *nuclear magnetic resonance* (n.m.r.), while for electrons it is called *electron spin resonance* (e.s.r.) or, sometimes, *electron paramagnetic resonance* (e.p.r.).

Experimentally there is a choice of two arrangements. We might either apply a fixed magnetic field to a set of identical nuclei so that their Larmor frequencies are all, say, 100 MHz; if the frequency of the radiation beam is then swept over a range including 100 MHz, resonance absorption will occur at precisely that frequency. On the other hand, we could bathe the nuclei in radiation at a fixed frequency of 100 MHz and sweep the applied field over a range until absorption occurs.

The probability of transitions occurring from one spin state to another is directly proportional to the population of the state from which the transition takes place. We have seen in the previous section that these populations are very nearly equal, and so during resonance, upward and downward transitions are induced to almost the same extent. However, while the lower state is more populated than the upper (e.g. at equilibrium in the absence of radiation), upward transitions predominate slightly, and a net (but very small) absorption of energy occurs from the radiation beam. When the populations become equal, upward and downward transitions are equally likely, no further absorption can take place, and the system is said to be *saturated*. The equilibrium populations can be re-established if the system loses its absorbed energy; this it cannot do spontaneously, but only as a result of interaction with radiation or with fluctuations

in surrounding magnetic fields of the appropriate frequency. The emitted energy can be collected and displayed as an emission spectrum which, since the emission is induced and not spontaneous, is called the *nuclear induction spectrum*.

7.2 NUCLEAR MAGNETIC RESONANCE SPECTROSCOPY: HYDROGEN NUCLEI

We have seen that a particular chemical nucleus placed in a magnetic field gives rise to a resonance absorption of energy from a beam of radiation, the resonance frequency being characteristic of the nucleus and of the strength of the applied field (some data have already been referred to in Table 7.1). Thus n.m.r. techniques may be used to detect the presence of particular nuclei in a compound and, since for a given nuclear species the strength of the n.m.r. signal is directly proportional to the number of resonating nuclei, to estimate them quantitatively. However, an n.m.r. spectrometer is an expensive instrument, and there are many simpler and cheaper methods available to detect the presence or absence of a particular atom in a molecule. Two other characteristics of n.m.r. spectra which have not so far been mentioned make the technique far more powerful and useful; these are the *chemical shift* and the *coupling constant*, which we shall discuss in the following sections.

The vast majority of substances of interest to chemists contain hydrogen atoms and, as this nucleus has one of the strongest resonances, it is not surprising that n.m.r. has found its widest application to these substances. When discussing chemical shifts and nuclear coupling it is convenient to use one type of nucleus as an example, although all spinning nuclei show these phenomena, and in what follows we shall consider the spectra of hydrogen-containing substances only, leaving discussion of other nuclei to Sec. 7.3.

7.2.1 The Chemical Shift

Up to now we have considered the behaviour of an isolated nucleus in an applied field. Such a situation is not, of course, realizable in practice since all nuclei are associated with electrons in atoms and molecules. When placed in a magnetic field the surrounding electron cloud tends to circulate in such a direction as to produce a field *opposing* that applied (so-called diamagnetic circulation), as shown for a single atom in Fig. 7.8. Plainly the total field experienced by the nucleus is:

$$B_{\text{effective}} = B_{\text{applied}} - B_{\text{induced}}$$

and, since the induced field is directly proportional to the applied field

$$B_{\text{induced}} = \sigma B_{\text{applied}}$$

where σ is a constant, we have:

$$B_{\text{effective}} = B_0(1 - \sigma) \tag{7.13}$$

where B_0 is the applied magnetic field. (Note that we here use the n.m.r. spectroscopist's normal notation of B_0 for the applied field, rather than B_z used earlier, since henceforth we shall not be concerned with the details of spin vector interaction with the field.) Thus the nucleus can be said to be *shielded* from the applied field by diamagnetic electronic circulation. The extent of the shielding will be constant for a given atom in isolation, but will vary with the electron density about an atom in a molecule; thus we may generalize Eq. (7.13) by writing:

$$B_i = B_0(1 - \sigma_i) \tag{7.14}$$

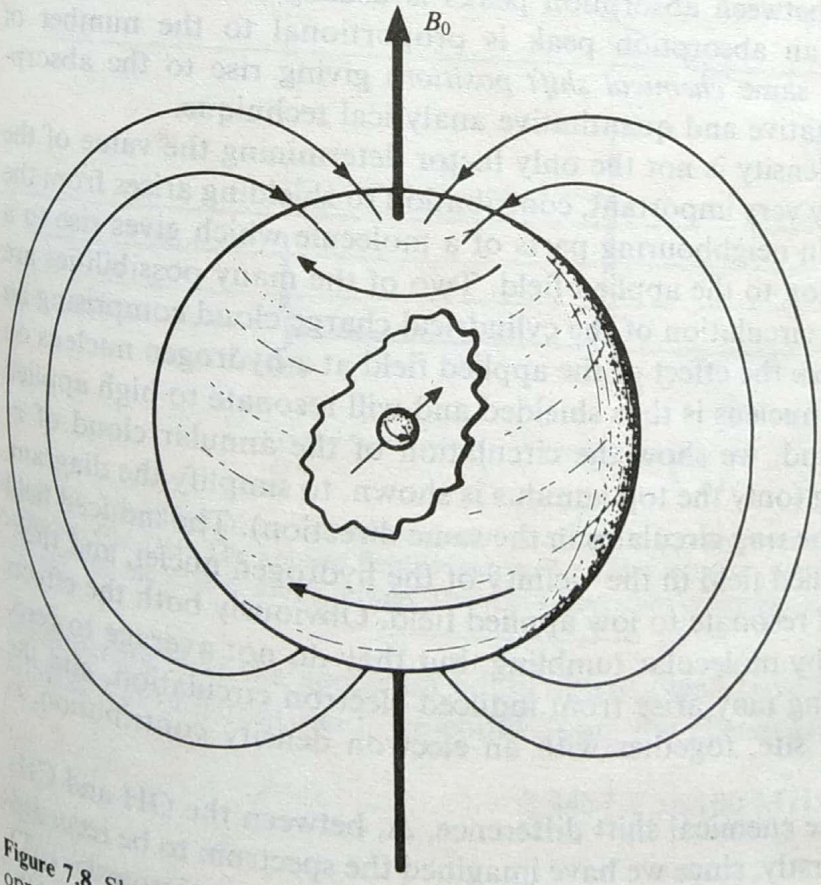

Figure 7.8 Showing the field, produced by diamagnetic circulation of the electron cloud about a nucleus, which opposes the applied field B_0.

where B_i is the field experienced by a particular nucleus i whose shielding constant is σ_i. As an example, since we know that oxygen is a much better electron acceptor than carbon (since oxygen has the greater electronegativity), then the electron density about the hydrogen atom in C—H bonds should be considerably higher than in O—H bonds. We would thus expect $\sigma_{CH} > \sigma_{OH}$ and hence

$$B_{CH} = B_0(1 - \sigma_{CH}) < B_{OH} = B_0(1 - \sigma_{OH})$$

Thus the field experienced by the hydrogen nucleus in O—H bonds is greater than that at the same nucleus in C—H bonds and, for a given applied field, the CH hydrogen nucleus will precess with a smaller Larmor frequency than that of OH. Put conversely, in order to come to resonance with radiation of a particular frequency (for example 100 MHz), a CH hydrogen requires a greater applied field than OH.

The effect of a steadily increasing field on the energy levels of the CH_3 and OH hydrogens in CH_3OH is shown in Fig. 7.9. The OH hydrogen nucleus, having a smaller shielding constant, experiences a greater field; hence its energy levels are more widely spaced than those of the more shielded CH_3 nuclei at any given applied field. If the system is irradiated with a beam of radiation at, say, 100 MHz while the applied field is increased from zero, the OH nucleus will come into resonance first and absorb energy from the beam, the CH_3 nuclei absorbing at a higher field. This is shown in the spectrum of methanol, CH_3OH, at the foot of the figure. The fact that the ratio of the absorption intensities (strictly the ratio of the areas under the peaks) is 1 : 3 immediately allows us to identify the smaller peak with the single hydrogen nucleus in the OH group, the larger with the CH_3 group. Since neither carbon nor oxygen have nuclei with spin, they do not contribute to the spectrum.

Two very important facets of n.m.r. spectroscopy appear in Fig. 7.9: (1) identical nuclei (that is H nuclei) give rise to different absorption *positions* when in different *chemical* surroundings (for this reason the separation between absorption peaks is usually referred to as their *chemical shift*) and (2) the *area* of an absorption peak is proportional to the number of *equivalent* nuclei (i.e. nuclei with the same *chemical shift position*) giving rise to the absorption. We see here the basis of a qualitative and quantitative analytical technique.

It should be noted that electron density is not the only factor determining the value of the shielding constant. Another, frequently very important, contribution to shielding arises from the field-induced circulation of electrons in neighbouring parts of a molecule which gives rise to a small magnetic field acting in opposition to the applied field. Two of the many possibilities are shown in Fig. 7.10. In Fig. 7.10(*a*) the circulation of the cylindrical charge cloud comprising an acetylenic triple bond is shown to *reduce* the effect of the applied field at a hydrogen nucleus on the axis of the circulating charge. The nucleus is thus shielded and will resonate to high applied field. In Fig. 7.10(*b*), on the other hand, we show the circulation of the annular cloud of π-orbital electrons around a benzene ring (only the top annulus is shown, to simplify the diagram, but the identical annulus underneath the ring circulates in the same direction). The induced field is here in the *same direction* as the applied field in the vicinity of the hydrogen nuclei, and these nuclei are consequently deshielded and resonate to low applied field. Obviously both the effects noted here will be somewhat reduced by molecular tumbling, but they do not average to zero. Thus both shielding and deshielding may arise from induced electron circulation, and the total of such effects at any particular site, together with an electron density contribution, is included in the shielding constant σ.

There are several ways in which the chemical shift difference, Δ, between the OH and CH_3 signals of Fig. 7.9 may be expressed. Firstly, since we have imagined the spectrum to be recorded by varying the applied field, we could attach a tesla scale (or, rather, a microtesla (μT) scale, since the separation is very small) to the spectrum, and observe that $\Delta = 3.26\ \mu T$. Or,

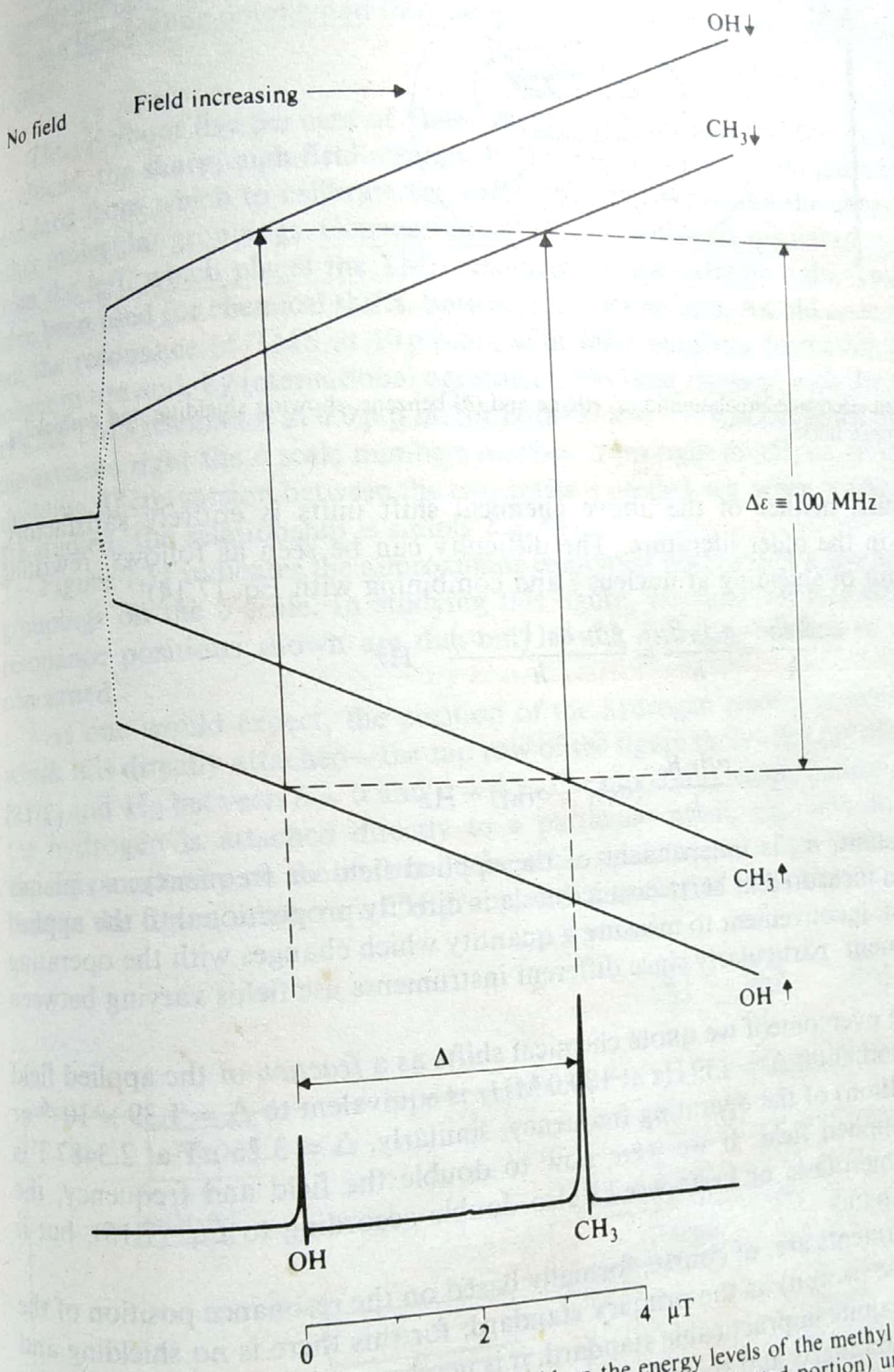

Figure 7.9 The effect of an applied magnetic field on the energy levels of the methyl and hydroxyl nuclei of methanol, CH_3OH. The applied field is increased rapidly initially (dotted portion) until near resonance at 2.3487 T and then the increase is much slower. The n.m.r. spectrum of methanol is shown at the foot of the figure.

remembering that the spectrum could equally well have been obtained by varying the applied frequency at constant field, we could quote the chemical shift difference in hertz as follows:

$$2.3487\ \text{T} \equiv 100\ \text{MHz}$$

Hence:

$$3.26\ \mu\text{T} \equiv 139\ \text{Hz} = \Delta$$

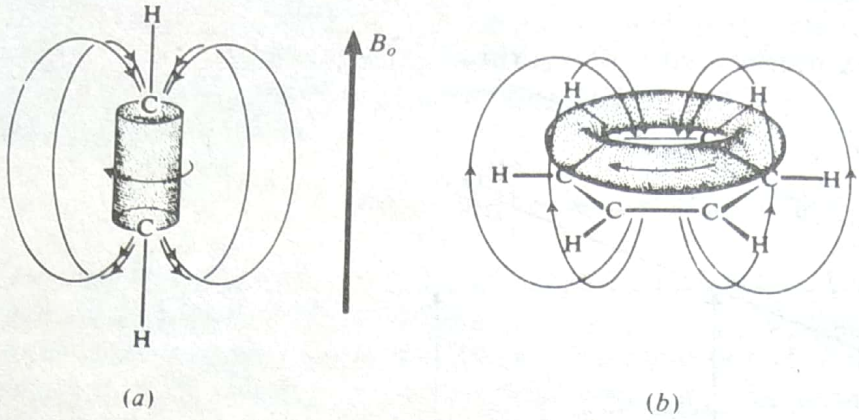

Figure 7.10 The field-induced electronic circulation in (*a*) ethyne and (*b*) benzene, showing shielding and deshielding, respectively, at nearby hydrogen nuclei.

In practice, however, neither of the above chemical shift units is entirely satisfactory, although both appear in the older literature. The difficulty can be seen as follows: rewriting Eq. (7.9) to take account of shielding at nucleus i and combining with Eq. (7.14):

$$\frac{\Delta E_i}{h} = \frac{g\beta_N B_i}{h} = \frac{g\beta_N B_0(1-\sigma_i)}{h} \quad \text{Hz}$$

and so, in hertz:

$$\Delta = \frac{g\beta_N B_0}{h}(\sigma_{CH} - \sigma_{OH}) \quad \text{Hz} \tag{7.15}$$

Now the shielding constant, σ_i, is independent of the applied field or frequency, so plainly chemical shift separation measured in hertz or microtesla is directly proportional to the applied field, B_0: it is, at the least, inconvenient to measure a quantity which changes with the operating conditions of the instrument, particularly since different instruments use fields varying between 0.6 and 15 tesla.

The difficulty can be overcome if we quote chemical shifts as a *fraction* of the applied field or frequency. Thus for methanol, $\Delta = 139$ Hz at 100.0 MHz is equivalent to $\Delta = 1.39 \times 10^{-6}$ or 1.39 p.p.m. (parts per million) of the operating frequency; similarly, $\Delta = 3.26\ \mu$T at 2.3487 T is also 1.39 p.p.m. of the applied field. If we were now to double the field and frequency, the separation expressed in microtesla or hertz would also double according to Eq. (7.15), but it would still be just 1.39 p.p.m.

Chemical shift measurments are, of course, formally based on the resonance position of the bare hydrogen nucleus (the proton) as the primary standard; for this there is no shielding and hence $\sigma = 0$. Since this is a quite impracticable standard, it is necessary to choose some reference substance as a secondary standard and to measure the resonance positions of other hydrogen nuclei from this in parts per million; the substance now almost universally selected for hydrogen resonances is tetramethyl silane, $Si(CH_3)_4$, usually abbreviated to TMS. Since TMS is immiscible with water, in aqueous solutions the salt $(CH_3)_3SiCH_2CH_2CH_2SO_3Na$ is used; its methyl protons resonate at exactly the same position as those of TMS. Both of these substances are also excellent references for ^{13}C spectra.

Tetramethyl silane has several advantages over other substances which have been used as standards:

1. Its resonance is sharp and intense since all 12 hydrogen nuclei are equivalent (i.e. have the same chemical environment) and hence absorb at exactly the same position.

2. Its resonance position is to high field of almost all other hydrogen resonances in organic molecules (that is σ_{TMS} is large) and hence can be easily recognized.
3. It is a low boiling point liquid (b.p. 27 °C) so can be readily removed from most samples after use.

Thus if about five per cent of TMS is added to a sample and the complete n.m.r. spectrum produced, the sharp, high-field resonance of the TMS is easily recognized and can be used as a standard from which to calibrate the spectrum and to measure the chemical shift positions of other molecular groupings. Conventionally n.m.r. spectra are displayed with the field increasing from the left, which places the TMS resonance to the extreme right. Two measurement scales have been used for chemical shifts, both in parts per million. An old scale, the τ scale, arbitrarily put the resonance of TMS at 10 p.p.m., with scale numbers decreasing to the left. This is no longer in use and, by international agreement, has been replaced with the so-called δ scale which sets the TMS resonance at 0.0 p.p.m. for both ^1H and ^{13}C spectra. Since the TMS resonance is at the extreme right the δ scale numbers increase from right to left, i.e. in the direction of weaker shielding. If conversion between the two scales is needed, e.g. when spectra in the older literature are studied, the relationship is simply $\delta = 10 - \tau$.

Figure 7.11 indicates the approximate resonance positions of a few molecules and molecular groupings on the δ scale. In studying this figure, we must not lose sight of the fact that the resonance positions shown are due only to the *hydrogen* nucleus in the molecule or group concerned.

As one would expect, the position of the hydrogen resonance depends upon the atom to which it is directly attached—the top row of the figure shows this for the series CH_4, NH_3, PH_3, SiH_4, and H_2 between $\delta = 0$ and $\delta = 4.2$. Far more important, however, is the fact that, when the hydrogen is attached directly to a particular atom, e.g. carbon, its resonance position depends markedly on the nature of the *other* substituents to that atom. Most of the remaining data in the figure relate to a CH group with a variety of substituents; we may note that, in the

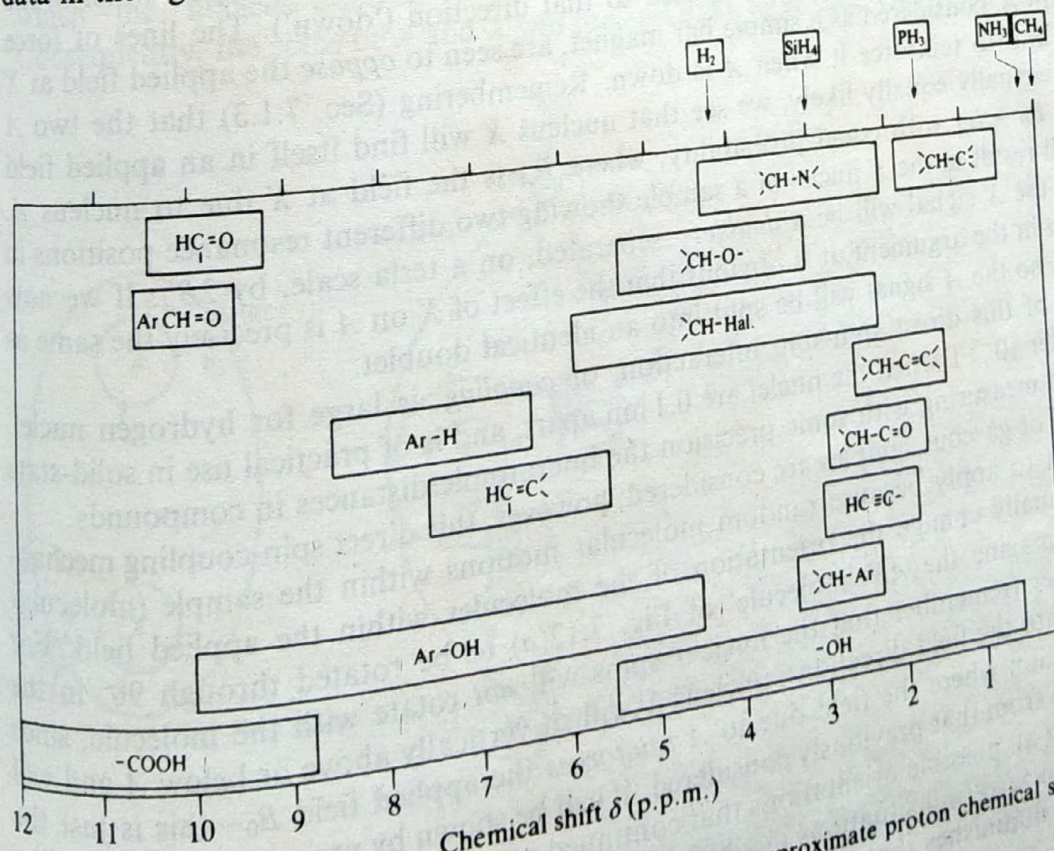

Figure 7.11 Showing the δ-scale of chemical shift values and the approximate proton chemical shifts of some simple molecules and groups.

series CH—C (at around 1 p.p.m.), CH—N (2–4 p.p.m.), and CH—O (3–5 p.p.m.), it is evident that the increasing electronegativity of the substituent progressively withdraws electrons from the neighbourhood of the hydrogen, thus reducing the shielding of the nucleus and allowing it to resonate at lower field (and higher δ number). A double- or triple-bonded substituent has a similar but smaller effect. We have already mentioned the strong deshielding effect produced by electron circulation in an aromatic ring and we note here that the resonance of a ring proton falls at around 7–8 p.p.m. The very wide range of observed resonances for OH and COOH groups occurs because the proton shielding is much affected by hydrogen bonding in these groups, so solvent, concentration, and even temperature changes can produce marked differences in their δ-values.

Figure 7.11 shows only a very small part of the huge mass of n.m.r. data available—much more is to be found in the very detailed tables and charts given in specialized texts, such as that by Williams and Fleming listed in the bibliography at the end of the chapter. Suffice it here to say that, combining detailed knowledge of chemical shift positions with the fact that the area of each resonance in the spectrum is proportional to the number of hydrogen nuclei contributing to that resonance, we see that n.m.r. is an excellent technique for both quantitative and qualitative group analysis in organic chemistry. After the following sections, where we discuss the phenomenon of energy coupling between nuclei, we shall see that the usefulness of n.m.r. extends further to the determination of the structure and configuration of molecules.

7.2.2 The Coupling Constant

Suppose that two hydrogen nuclei in different parts of a solid, e.g. a crystal lattice, are sufficiently close together in space that they exert an appreciable magnetic effect on each other—in n.m.r. terms 'appreciable' means 0.01 μT or more. We show such a case in Fig. 7.12 for two nuclei labelled A and X. Here we ignore the spin direction of X since this is immaterial for the moment, but we show the two possible directions of the z component of A's spin, either in the field direction (conventionally 'up') or opposed to that direction ('down'). The lines of force originating from A, considered as a simple bar magnet, are seen to *oppose* the applied field at X when A is up and to reinforce it when A is down. Remembering (Sec. 7.1.3) that the two A directions are virtually equally likely, we see that nucleus X will find itself in an applied field $B_0 + B_A$ or in $B_0 - B_A$ with equal probability, where B_A is the field at X due to nucleus A. Clearly this will result in the X nuclei of a sample showing two different resonance positions in the spectrum—the X signal will be a *doublet*—separated, on a tesla scale, by $2B_A$. If we now include X's spin in the argument, it is obvious that the effect of X on A is precisely the same as that of A on X, so the A signal will be split into an identical doublet.

The extent of this direct spin-spin interaction, or *coupling*, is large for hydrogen nuclei, being of the order 10^{-4} T when the nuclei are 0.1 nm apart, and is of practical use in solid-state n.m.r. spectra in measuring with some precision the interatomic distances in compounds.

When liquid or gaseous samples are considered, however, this direct spin-coupling mechanism is found not to apply because random molecular motions within the sample (molecular tumbling) continually change the orientation of the molecules within the applied field. For example, if we imagine the AX 'molecule' of Fig. 7.12(a) to be rotated through 90° in the plane of the paper (remember that the nuclear spins will *not* rotate with the molecule, since they are locked into the field direction), nucleus X will sit vertically above or below A and will thus be in a position where the field due to A *reinforces* the applied field B_0—this is just the opposite situation from that previously considered. It can be shown by proper integration of the effect of A on X at all possible orientations that continued rotation of the molecule averages the coupling exactly to zero—all situations in which A reinforces the field at X are just balanced by all those where it diminishes that field.

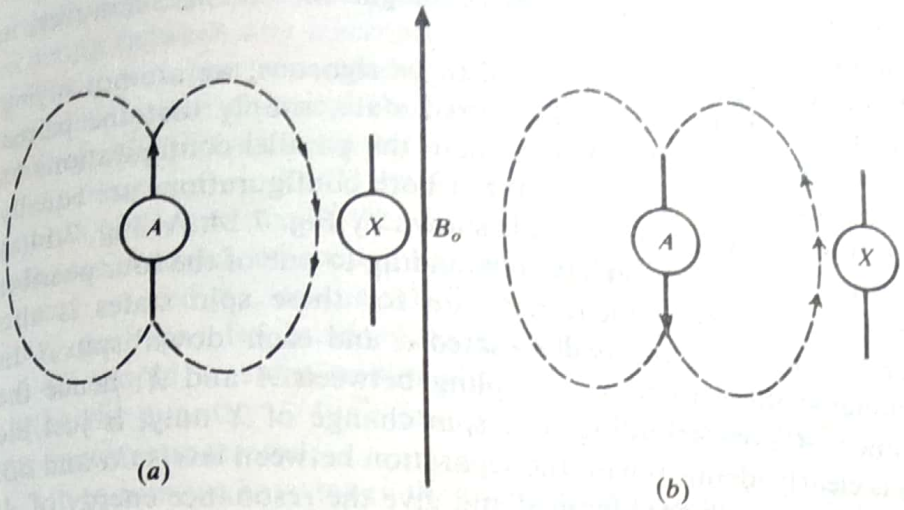

Figure 7.12 The direct coupling of nuclear spins. In (*a*) the spin of *A* decreases the net magnetic field at *X*, while in (*b*) the field at *X* is increased.

Nonetheless, the n.m.r. spectra of liquids do show the phenomonen of coupling but the effect is very much smaller (by a factor of 10^2–10^4 than that observed for direct coupling in solids); clearly a different mechanism is involved. Consider first Fig. 7.13(*a*) which shows two hydrogen nuclei joined by a pair of bonding electrons, as in the hydrogen molecule. To a first approximation we can assume that each electron 'belongs' to a particular nucleus, so we associate electron (*a*) with nucleus *A* and electron (*x*) with nucleus *X*. Plainly the most stable state energetically is that in which the electronic magnetic dipole is opposed to that of its own nucleus, but theories of chemical bonding tell us that the electrons, which occupy the same orbital, will have their spins opposed also, and so we see that the most stable state will be that in which the nucleus–electron–electron–nucleus spins alternate as shown in the figure. Consequently, the spins of *A* and *X* will preferentially be paired. This is similar to the situation

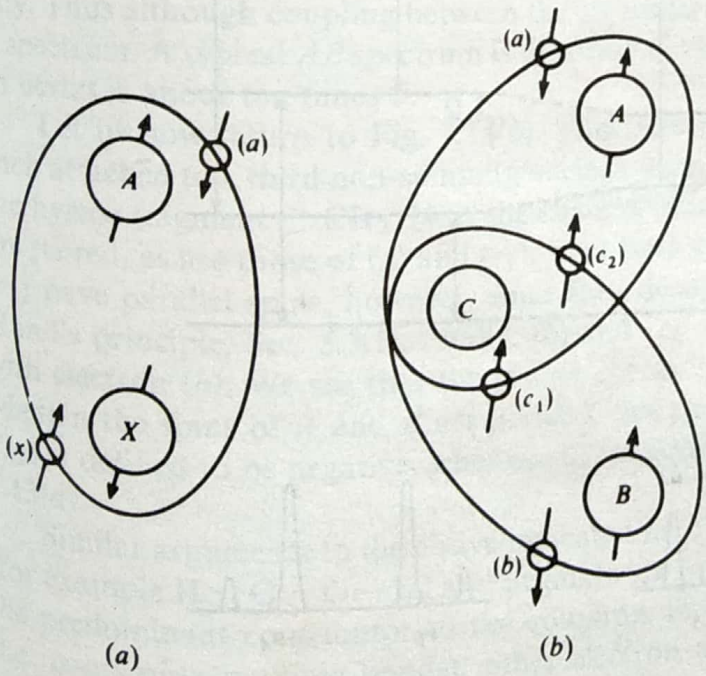

Figure 7.13 The coupling of nuclear spins via bonding electrons for (*a*) directly bonded atoms and (*b*) atoms bound to a third atom having no spin.

found for the 'across-space' effect, but is several orders of magnitude smaller; however, it represents coupling between the nuclei.

Note carefully that the above argument is not intended to be rigorous; we are not saying that the spins of A and X are immutably fixed in the paired state, simply that the paired configurations $\uparrow\downarrow$ and $\downarrow\uparrow$ are very slightly lower in energy than the parallel configurations $\uparrow\uparrow$ and $\downarrow\downarrow$. The energy difference is so minute (some 10^{-32} J) that both configurations are equally likely to occur. The effect which this has on the spectrum is shown by Fig. 7.14. At Fig. 7.14(a) we show the four energy levels of the AX system, each corresponding to one of the four possible spin combinations, $\uparrow\downarrow$, $\uparrow\uparrow$, $\downarrow\downarrow$ and $\downarrow\uparrow$; a convenient notation for these spin states is also indicated on the diagram, whereby each 'up' spin is designated α and each 'down' spin β. In this part of the diagram we imagine there to be no coupling between A and X; hence the separation between levels $\alpha\alpha$ and $\alpha\beta$, corresponding to a spin change of X only, is just the resonance energy of X, and this is clearly identical with the separation between levels $\beta\alpha$ and $\beta\beta$. Similarly, the separations $\alpha\alpha$–$\beta\alpha$ and $\alpha\beta$–$\beta\beta$ are identical and give the resonance energy of A. Transitions between the various levels give rise to two spectral lines, one at each of the chemical shift positions of A and of X, desinated ν_A and ν_X.

When coupling occurs we know that the levels $\alpha\alpha$ and $\beta\beta$ are destabilized, and that $\alpha\beta$ and $\beta\alpha$ are stabilized; this is shown in Fig. 7.14(b), where the amount of the energy change is symbolized as $J/4$—the convenience of this will become clear shortly. Now the two possible X transitions have different energies: there is $\alpha\alpha \leftrightarrow \alpha\beta$ which is smaller than in Fig. 7.14(a) by $\frac{1}{2}J$, and $\beta\alpha \leftrightarrow \beta\beta$, higher by $\frac{1}{2}J$; hence one spectral line appears $\frac{1}{2}J$ above ν_X and another $\frac{1}{2}J$ below, the separation between these two lines being just J (hence the convenience of defining the stabilization and destabilization as $J/4$ above). Similarly, the A transitions will be split into an identical doublet. The 'legs' of the doublet will be the same intensity since (1) all spin states are

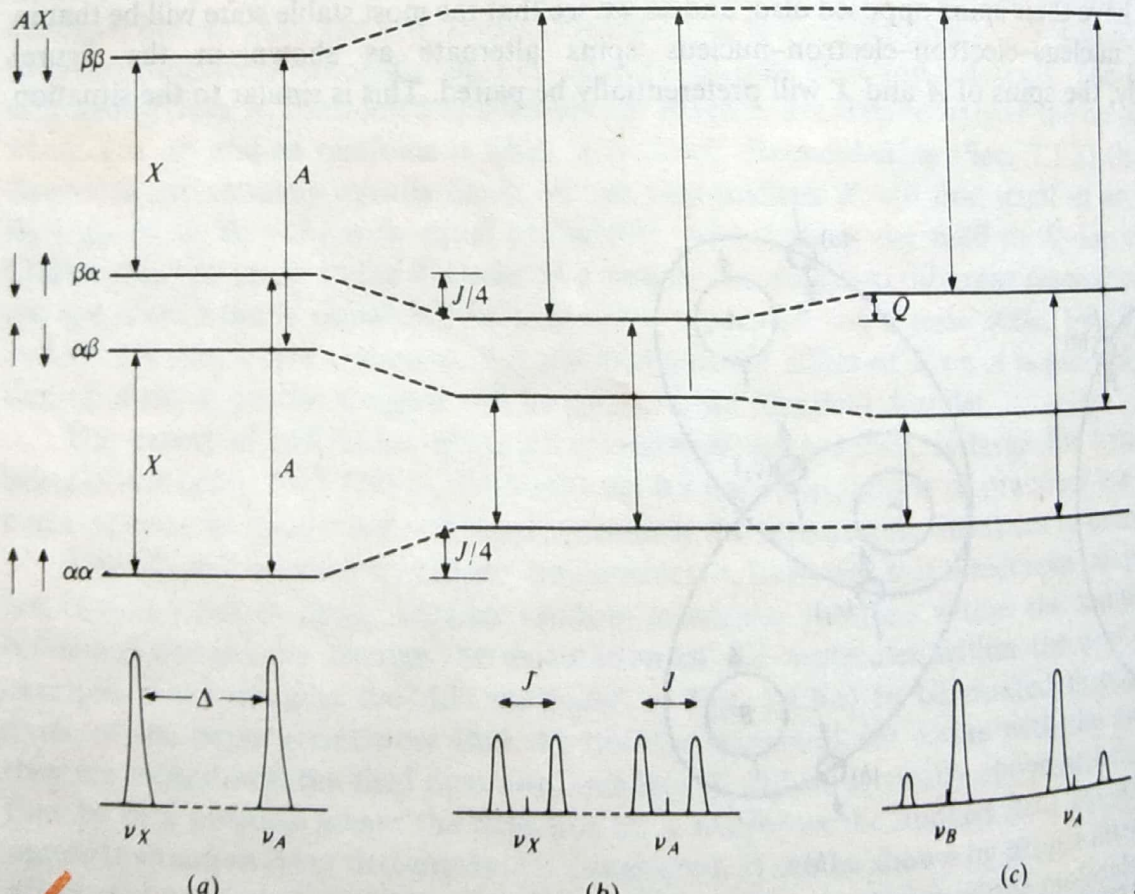

Figure 7.14 To illustrate the effect of coupling between two nuclei. At (a) coupling is ignored, at (b) the coupling is taken to be small compared with the chemical shift, and at (c) the coupling is large compared with the chemical shift.

virtually equally likely and (2) detailed calculation shows that the probabilities of transitions occurring between any levels are identical. Thus we arrive at an AX spectrum: a pair of 1 : 1 doublets, each pair separated by the coupling constant J and the midpoints of the doublets separated by the chemical shift difference Δ. Since J is observed to be a field-independent quantity, it is conveniently expressed in hertz rather than in parts per million like δ.

At this point we should emphasize that Fig. 7.14 is by no means drawn to scale. If A and X are both hydrogen nuclei, then in Figure 7.14(a) the transitions labelled X and A represent the resonance energies of such nuclei in, say, a 2.5 T field, i.e. some 100 MHz. The separation between $\alpha\beta$ and $\beta\alpha$, on the other hand, represents the chemical shift difference Δ between ν_A and ν_X, perhaps a few hundred hertz. Thus if the diagram were to scale, the distance between $\alpha\alpha$ and $\alpha\beta$ should be some million times greater than that between $\alpha\beta$ and $\beta\alpha$. Turning to Fig. 7.14(b), the quantity $J/4$ is a few hertz only, so the displacements of the various energies have been much exaggerated.

Up to now we have taken the chemical shift difference of A and X (some 100 Hz) to be large compared with the coupling constant J (a few hertz). In Fig. 7.14(c) we show what happens when the chemical shift difference decreases, i.e. when the levels $\alpha\beta$ and $\beta\alpha$ are assumed to be closer together than shown. It is a well-known fact in quantum mechanics that energy levels of the same symmetry, as are $\alpha\beta$ and $\beta\alpha$, tend to repel each other if they become close, while those of different symmetry, like $\alpha\alpha$ and $\beta\beta$, are not affected. If both $\alpha\beta$ and $\beta\alpha$ are repelled by an amount Q, as shown on the diagram, then clearly both X transitions are decreased in energy by Q, while both A transitions are increased by the same amount. The result is to push the spectral lines apart so that the chemical shift positions, ν_A and ν_X, are no longer at the midpoints of their respective doublets. Actually in the figure we have relabelled the nuclei A and B instead of A and X: this is conventional notation in n.m.r. spectroscopy, where letters close together in the alphabet are used to indicate nuclei whose chemical shift difference is small, and vice versa.

One further effect of a small chemical shift difference is illustrated in Fig. 7.14(c); this is that, although the populations of the levels are unaffected by the perturbation Q, the relative transition probabilities are very much affected, and detailed calculations show that the result is for the centre lines of the AB spectrum to gain intensity at the expense of the outer. In the limit when the chemical shift difference becomes zero (A_2 system instead of AB, since A and B become identical), the centre lines coalesce into one and the outer lines have vanishing intensity. Thus although coupling between the A_2 nuclei certainly exists, its effect is not observable in a spectrum. A typical AB spectrum is illustrated in Fig. 7.15 where it is evident that Δ (measured in hertz) is about ten times J.

Let us now return to Fig. 7.13(b). This shows the coupling of hydrogen nuclei which are each attached to a third non-spinning nucleus, such as carbon; an example of this situation is the methylene fragment $>CH_2$. Now the chain of reasoning runs as follows: the spins of A and (a) are paired, as are those of (a) and (c_1), since both of the latter occupy the same orbital; (c_1) and (c_2) have parallel spins, however, since they occupy degenerate orbitals in the same atom (cf. Hund's principle, Sec. 5.3.1); finally, (b) and (c_2) are paired and nucleus B has its spin paired with electron (b). We see that the lowest energy state, according to this electron path, is that wherein the spins of A and B are *parallel*, not paired. In this situation the coupling constant, J_{AB}, is defined to be negative, whereas it is defined positive for the previous case shown in Fig. 7.13(a).

Similar arguments to the above indicate that J is again positive for coupling via three bonds (for example H—C—C—H) and negative via four, etc., provided this type of electron path is the predominant contributor to the coupling; in some systems, particularly unsaturated ones (i.e. containing multiple bonds), other electron paths may become important. However, the magnitude of the coupling constant attenuates rapidly with increasing number of bonds; thus for H_2 the coupling (measured indirectly from the spectrum of HD) is some 240 Hz, for the

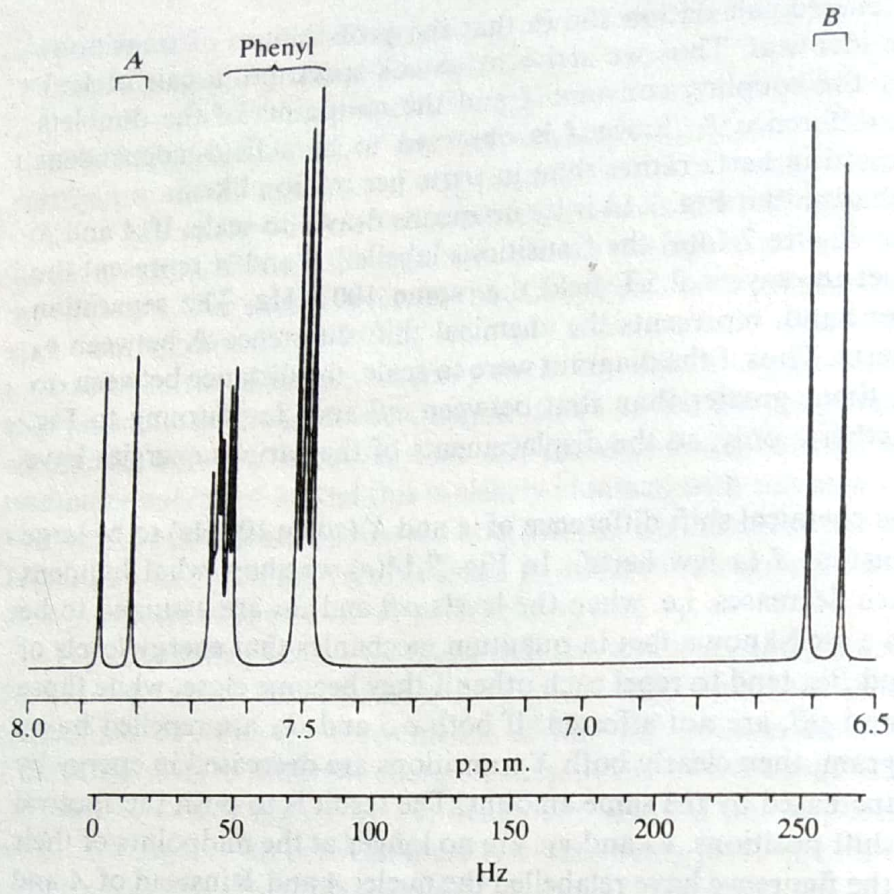

Figure 7.15 Part of the n.m.r. spectrum of ethyl cinnamate, $C_6H_5CH{=}CH.COOC_2H_5$, showing the typical *AB* pattern of the olefinic hydrogens. The resonances in the centre are due to the phenyl group; the ethyl resonance is off the scale to the right. (*Thanks are due to Mr A. Taylor of the University of York for this spectrum.*)

H—C—H fragment (e.g. in methane) it is some 12 Hz, for H—C—C—H (e.g. in ethanol, CH_3CH_2OH) it is 7 Hz and for H—C—C—C—H it is on the present limit of measurement, 0.5 Hz or less. However, in unsaturated molecules, in which electrons occupy orbitals extending over more than two nuclei and are thus more mobile, the couplings are somewhat larger and have been observed over more than four bonds.

It is not usually easy to determine the sign of a coupling constant experimentally, but where such data exist they are often in good agreement with the alternation theory outlined above. Further, calculations can be made predicting the magnitudes of certain couplings by applying quantum mechanical methods to the very diagrammatic approach of Fig. 7.13; these, too, are in generally good agreement with experimental values.

7.2.3 Coupling between Several Nuclei

So far we have considered the effect of coupling between two hydrogen nuclei only, but such nuclei often occur in molecules as groups, particularly CH_3 and CH_2 groups. We turn now to consider coupling between groups, using the ethyl fragment, CH_3CH_2, as our example.

In the ethyl fragment the three hydrogens of the methyl (CH_3) group have the same chemical shift since all the CH bonds are identical and the shielding at each of the nuclei is the same. Such nuclei are called *chemically equivalent*. In the same way the two nuclei of the methylene ($-CH_2-$) group are chemically equivalent but their chemical shift is, of course, different from that of the methyl nuclei. Further, there is some freedom of rotation of the methyl group in this fragment and hence the interaction between the methyl and methylene nuclei is averaged to the same value—the coupling constant is the same between any methyl and any

methylene hydrogen. The nuclei in the methyl group (or the methylene group) are said to be *magnetically equivalent* as well as chemically equivalent. This property affords a considerable simplification of the overall spectrum because the *couplings within a group of magnetically and chemically equivalent nuclei do not affect the spectrum* and can be ignored, as in the case of A_2 considered earlier. In the present example, this means we can neglect coupling between the methyl hydrogens themselves, or between the two methylene hydrogens, and need consider only the coupling between a methyl and methylene nucleus. Since all the latter couplings are equal, as explained above, the system has just one J value to be considered. If the chemical shift between methyl and methylene is large, then we have a system A_3X_2 (where A is a CH_3 hydrogen nucleus and X a CH_2 nucleus) with a coupling constant J_{AX}.

When considering the spectrum resulting from an A_3X_2 system it is quite possible to construct an energy-level diagram analogous to that of Fig. 7.14 for the AX case. Such a diagram is complex, however, and it is much simpler to use another approach, which may be called the 'family tree' method; in this, coupling between grouped nuclei is considered stepwise.

Thus in Fig. 7.16(a) we start by imagining the A_3 and X_2 groups to be uncoupled, and hence as giving rise to one line each of intensity 3 and 2 units, respectively. When we let the A_3 group couple to just *one* of the X_2 pair, the A_3 line is split into a doublet, separation J_{AX}, each line having intensity $1\frac{1}{2}$ units. If now each leg of this doublet is considered to couple with the second X nucleus, each will be split into a doublet, separation J_{AX}, intensity $\frac{3}{4}$ unit. However, the inner line of each doublet will overlap, because the coupling is identical for both, so the overall spectrum will have the appearance of a *triplet*, intensity of each line $\frac{3}{4}$, $1\frac{1}{2}$, $\frac{3}{4}$ (i.e. a 1 : 2 : 1 triplet) with the coupling J_{AX} appearing twice in the spectrum.

The splitting of X_2 by coupling with A_3 proceeds similarly. Coupling to one A yields a 1 : 1 doublet, to the second a $\frac{1}{2} : 1 : \frac{1}{2}$ triplet, and to the third a $\frac{1}{4} : \frac{3}{4} : \frac{3}{4} : \frac{1}{4}$ quartet (i.e. a 1 : 3 : 3 : 1 quartet) with the coupling constant J repeated three times.

This argument is very readily generalized: a group of p equivalent nuclei splits a neighbouring group into $p + 1$ lines with intensities given by the pth line of Pascal's triangle:

$p = 1$			1		1	
$p = 2$		1		2		1
$p = 3$	1		3		3		1
$p = 4$	1	4		6		4	1

where each entry is obtained by summing the two numbers to its right and left in the line immediately above. Thus the two nuclei of the X_2 group split the A_3 resonance into $2 + 1 = 3$ lines, while the X_2 resonance is itself split into $3 + 1 = 4$ lines by the A_3 nuclei.

The family tree method thus predicts a quartet and triplet structure for the $-CH_2CH_3$ spectrum, the former having a total intensity of two units, the latter of three. Comparison with the spectrum of CH_3CH_2OH at the foot of Fig. 7.16 shows that this prediction is amply justified. It must be stressed, however, that if the chemical shift separation of the CH_3 and CH_2 resonances were to be decreased (forming an A_3B_2 system), e.g. by lowering the operating field of the instrument or by changing the nature of the substituent on the CH_3CH_2- group, then the family tree method becomes a successively poorer approximation to the observed spectrum. Already in the A_3X_2 spectrum of Fig. 7.16 the inner lines are seen to have a slightly enhanced intensity with respect to the outer (cf. the AB pattern of Fig. 7.14), even though the chemical shift separation is some 20 times the coupling constant. At smaller shifts not only is the intensity distortion increased but additional lines begin to appear, quite inexplicable with the

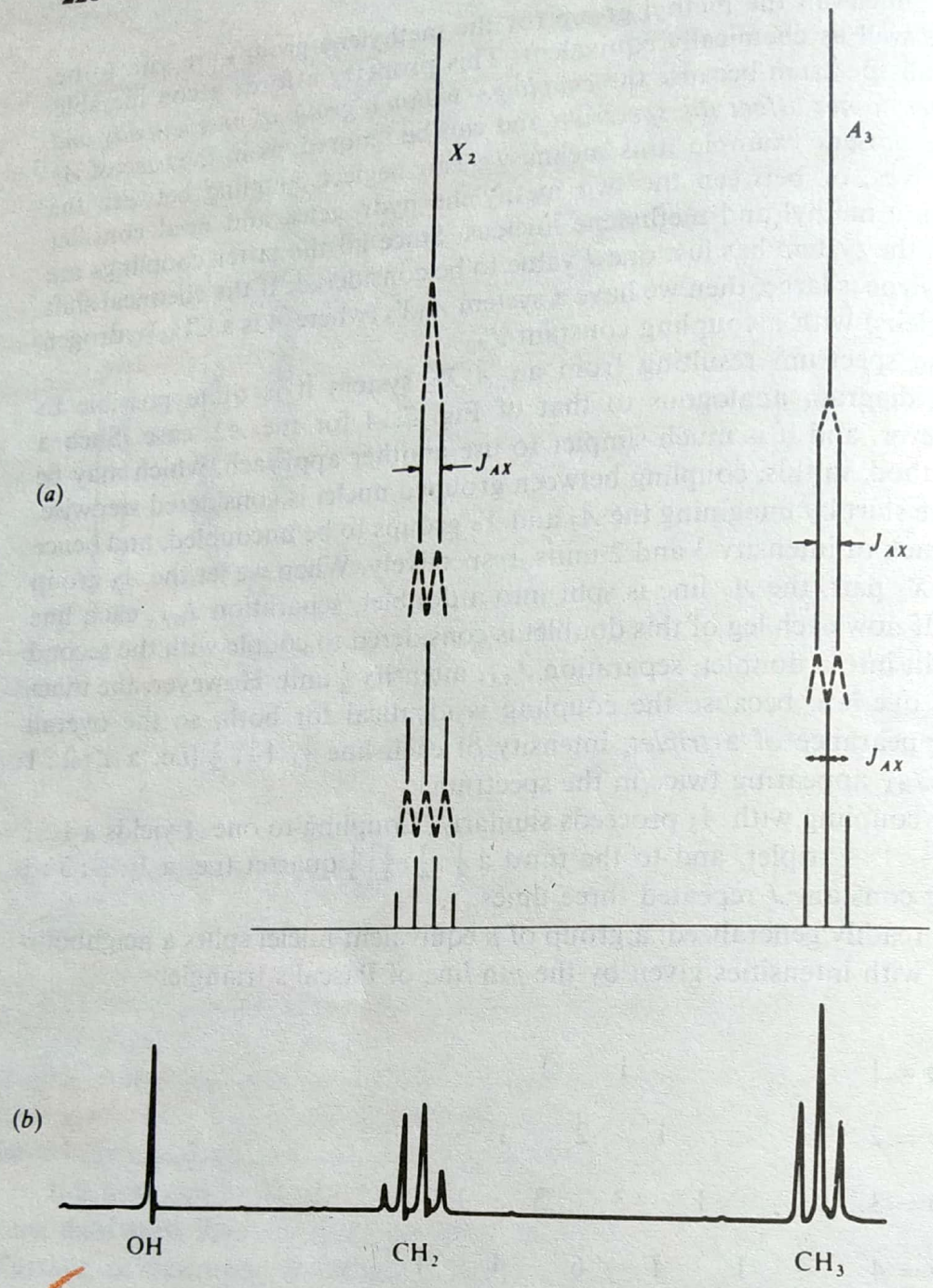

Figure 7.16 (*a*) A theoretical A_3X_2 spectrum and (*b*) the actual spectrum of ethanol, CH_3CH_2OH.

family tree method. Under these conditions accurate fit between theory and experiment is only possible by detailed calculation of the energy levels and transition probabilities for the system.

Some other typical coupling patterns are shown in Fig. 7.17. In Fig. 7.17(*a*) we see an A_2X_2 spectrum given by the substance cyanhydrin, $CNCH_2CH_2OH$. The methylene groups have different chemical shifts and so it is to be expected that coupling between them will split each resonance into a 1 : 2 : 1 triplet; this is to be observed in the spectrum. Other chemical structures giving rise to similar spectral patterns are 1,2-disubstituted benzenes, or five-membered unsaturated heterocyclic systems such as furan, although in such molecules the spectra are rather more complicated owing to additional couplings which arise between the nuclei. In Fig. 7.17(*b*) we show an A_6X spectrum arising from an isopropyl group, $(CH_3)_2CH-$. In this all six methyl hydrogens are equivalent and hence they split the lone methylene hydrogen into a septet, while they themselves are split into a doublet by the single nucleus. Such a pattern is easily recognizable even if the two outer lines of the septet are too weak to be observed, and is very characteristic.

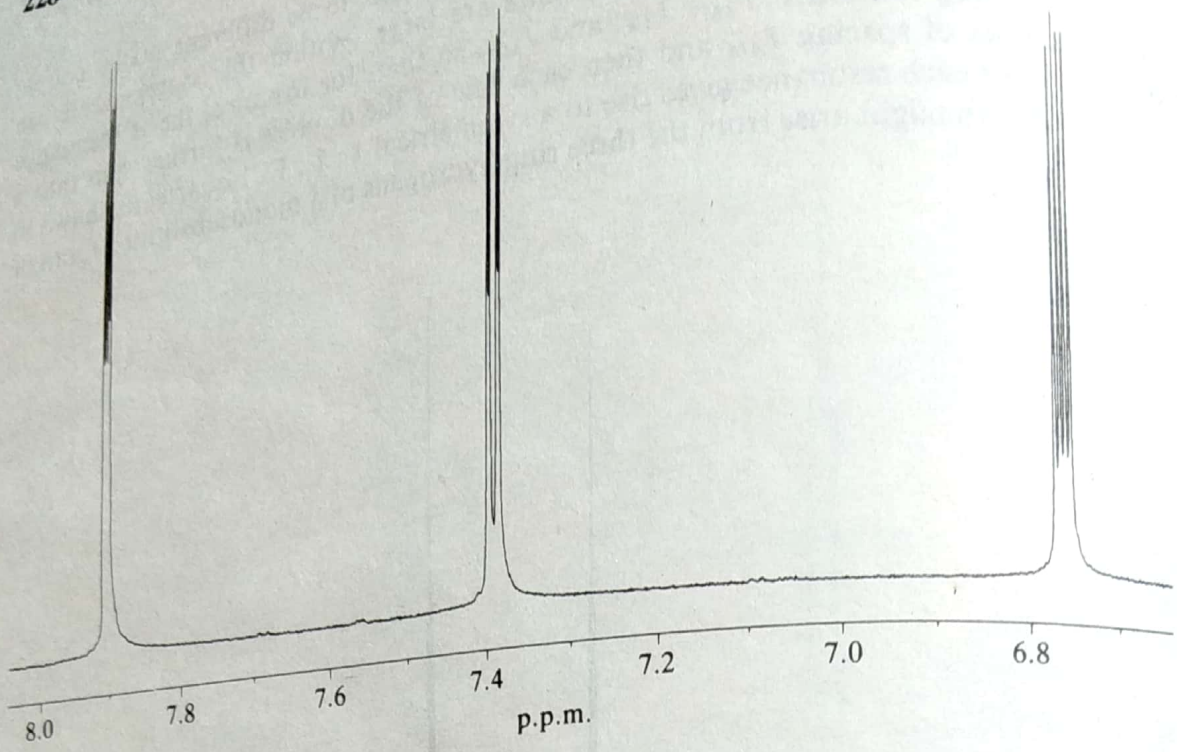

(*c*)

Figure 7.17 (*c*) Part of the n.m.r. spectrum of 2-furanoic acid, $\underbrace{OCH{=}CH.CH{=}C}.COOH$. Signals from the ring hydrogens only are shown, the resonance of the COOH being off-scale to the left. (*Thanks are due to Mr A. Taylor of the University of York for this spectrum.*)

similar molecule (in this example we show the spectrum of an α-furan) or it might be from a vinyl group $CH_2{=}CH-$, where again all three hydrogen nuclei have a different chemical shift.

These coupling patterns, like that for the CH_3CH_2- fragment, are considerably complicated if the chemical shift between coupled nuclei is small. Usually, however, the additional fine structure produced and the intensity perturbations do not prevent recognition of the overall pattern, particularly when some experience has been gained from studying actual spectra. The tremendous analytical value of such patterns is obvious since their recognition immediately gives information about the chemical groupings present in the molecule under examination. We discuss this aspect of n.m.r. spectra more fully in the next section.

7.2.4 Chemical Analysis by N.M.R. Techniques

In the preceding sections we have built up a picture of the application of n.m.r. to constitutional and structural studies. Thus the observation of the τ values of lines in a spectrum (or of the centres of multiplets if coupling is occurring) immediately indicates, with very little ambiguity, the types of hydrogen-containing groups within the molecule, while the relative intensities of the lines yield directly the proportions in which these groups occur.

Further, the multiplet structure of each group in the spectrum gives information on the number of hydrogen nuclei coupled to that group and in this way shows which groups are near neighbours in the molecule. Thus groups such as CH_3CH_2, $-CH_2CH_2-$, $(CH_3)_2CH-$, etc., can be instantly recognized from the n.m.r. spectrum.

As an example of the use and limitations of n.m.r. spectroscopy in analysis, consider the spectrum shown in Fig. 7.18. Resonances are centred at $\delta = 8.1$, 7.5, 4.4, and 1.3, the position of the former two and the coupling pattern of the latter two suggesting that they arise from a phenyl group (C_6H_5-) and an ethyl group (C_2H_5-), respectively. The integral trace on the spectrum shows these resonances to have relative intensities of 5 : 2 : 3 (the two phenyl

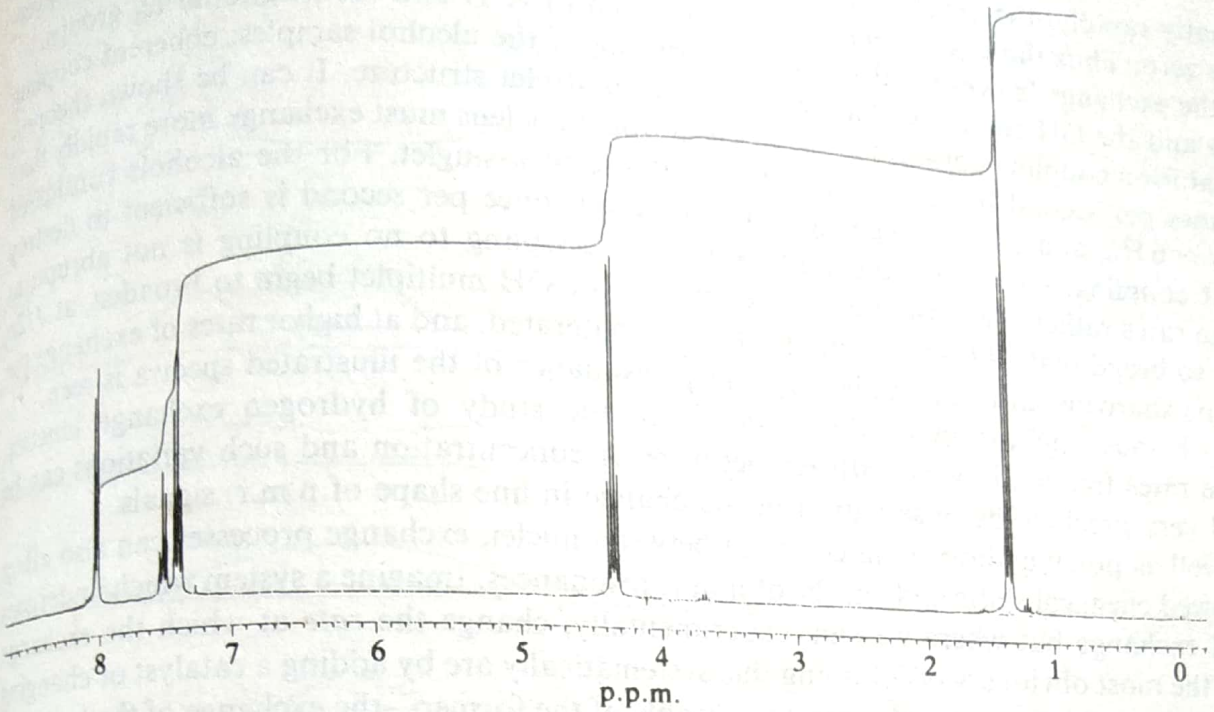

Figure 7.18 The n.m.r. spectrum of ethylbenzoate, $C_6H_5CO.OCH_2CH_3$, to illustrate the use of n.m.r. as an analytical technique. (*Thanks are due to Mr A. Taylor of the University of York for this spectrum.*)

resonances here being summed) so we know the phenyl and ethyl to be present in a 1 : 1 ratio. If we also know that the molecular formula of the substance is $C_9H_{10}O_2$, we can rapidly deduce that the resonances at $\delta = 8.1$ and 7.5 are due to hydrogen nuclei, respectively ortho and meta/para to a carbonyl group, while those at 4.4 and 1.3 are consistent with the grouping $CH_3CH_2.O.CO-$. The molecule is thus ethyl benzoate, $C_6H_5CO.O.CH_2CH_3$.

Note that the n.m.r. spectrum, while allowing us to deduce directly the presence of phenyl and ethyl groups, does not indicate the *presence* of groups not containing magnetic nuclei, in this case O and CO. However, once these groups are known to be present, either by determination of the molecular formula or by observation of the infra-red spectrum, then the n.m.r. spectrum does indicate their *position* in the molecule. Thus the coupling pattern shows clearly that the CH_3 and CH_2 groups are directly bound and not, for example, joined via O or CO ($CH_3.O.CH_2-$ or $CH_3.CO.CH_2-$) since in these latter configurations the coupling constant would be immeasurably small.

This very simple example serves to indicate the method of approach when using n.m.r. for analytical purposes. Of course, only in the simplest cases is a complete structural determination possible from the n.m.r. spectrum alone, but when taken in conjunction with other techniques, in particular infra-red spectroscopy, a great deal of useful structural information can usually be obtained about an unknown molecule.

7.2.5 Exchange Phenomena

The student may have been puzzled by one aspect of the alcohol spectra shown in Figs 7.9, 7.16, and 7.17; in these three spectra the resonance of the —OH hydrogen is shown as a single line whereas we might now expect it to be coupled with neighbouring CH_3, CH_2, or CH nuclei and hence have multiplet structure—quartet, triplet, or doublet, respectively. The reason it does not so couple is attributable to the fact that the hydroxyl hydrogen is readily exchanged with other hydrogen nuclei or ions in its vicinity; when this happens, the replacement hydrogen does not necessarily have the same spin direction as that being displaced and, if the exchange occurs

7.5 ELECTRON SPIN RESONANCE SPECTROSCOPY

7.5.1 Introduction

In Chapter 6 we saw that the majority of stable molecules are held together by bonds in which electron spins are paired; in this situation there is no net electron spin, no electronic magnetic moment, and hence no interaction between the electron spins and an applied magnetic field. On the other hand, some atoms and molecules contain one or more electrons with unpaired spins, and these are the substances which are expected to show *electron spin resonance* (e.s.r.) spectroscopy; since such substances are also paramagnetic, this type of spectroscopy is often referred to as *electron paramagnetic resonance* (e.p.r.).

Substances with unpaired electrons may either arise naturally or be produced artificially. In the first class come the three simple molecules, NO, O_2, and NO_2, and the ions of transition metals and their complexes, for example Fe^{3+}, $[Fe(CN)_6]^{3-}$, etc. These substances are stable and easily studied by e.s.r. Unstable paramagnetic materials, usually called *free radicals* or *radical ions*, may be formed either as intermediates in a chemical reaction or by irradiation of a 'normal' molecule with ultra-violet or X-ray radiation or with a beam of nuclear particles. Provided the lifetimes of such radicals are greater than about 10^{-6} s they may be studied by e.s.r. methods; species short-lived at room temperature may also be studied if they are produced at a low temperature, either in the solid state or trapped in a solid 'matrix' of a host material such as a solid inert gas. This is called *matrix isolation* and increases the lifetime of the trapped radical. Obviously, while there are many and various substances to which e.s.r. can be applied, the requirement for an unpaired electron means that the technique is generally less applicable than n.m.r.

When unpaired electrons exist in a substance their spins are aligned at random in the absence of a field. When placed in a magnetic field, however, they will each have a preferred direction and, since the spin quantum number of an electron is $\frac{1}{2}$, each can be thought of as spinning either clockwise or anticlockwise about the field direction. E.s.r. spectroscopy essentially measures the energy required to reverse the spin of an unpaired electron.

Virtually all the theory which we shall need in the discussion of e.s.r. spectra has been dealt with in preceding sections of this chapter; Sec. 7.1 is particularly relevant here, since it covers such matters as the electron's magnetic moment, its interaction with an applied magnetic field to give two energy levels, the populations of those levels, the Larmor precession, and relaxation process. In fact, with the exception of the magnitudes of some quantities, the whole of Sec. 7.1 can be carried straight over into the discussion of e.s.r. spectroscopy. Parts of Sec. 7.2, such as the remarks regarding spin-spin coupling, are also relevant, as we shall see.

As in all forms of spectroscopy, four properties of the spectral lines are of importance, viz. their intensity, width, position, and multiplet structure. The first two we can deal with quite briefly; the final pair merit separate sections.

The *intensity* of an e.s.r. absorption is proportional to the concentration of the free radical or paramagnetic material present. Thus we have immediately a technique for estimating the

amount of free radical present; the method is extraordinarily sensitive, in favourable cases some 10^{-13} mol of free radical being detectable.

The *width* of an e.s.r. resonance depends, as in the case of n.m.r., on the relaxation time of the spin state under study. Of the two possible relaxation processes, the spin-spin interaction is usually very efficient, unless the sample is extremely dilute, and gives a relaxation time of 10^{-6}–10^{-8} s; the spin-lattice relaxation is efficient at room temperature (some 10^{-6} s) but becomes progressively less so at reduced temperatures, often becoming several minutes at the temperature of liquid nitrogen. For most samples, then, we could choose 10^{-7} s as a typical relaxation time and, using this in the Heisenberg uncertainty relation of Eq. (1.11), we calculate a frequency uncertainty (line width) of $(2\pi\,\delta t)^{-1} \approx 1$ MHz. A shorter relaxation time will increase this width, and 10 MHz is not uncommon. Clearly this is a *much* wider spectral line than in the case of n.m.r., where we found a normal line width for a liquid to be some 0.1 Hz.

The wider e.s.r. lines have advantages and disadvantages. On the credit side, the homogeneity of the applied magnetic field is far less critical and where, for n.m.r., it is essential to use a magnetic field homogeneous to 1 in 10^8 over the sample, for e.s.r. a figure of 1 in 10^5 is adequate; this represents a considerable easing of manufacturing tolerances. On the debit side, however, broad-lined e.s.r. spectra mask any effects equivalent to the n.m.r. chemical shift. In addition, a broad line is more difficult to observe and measure than a sharp one and, for this reason, e.s.r. spectrometers nearly always operate in the derivative mode (see Chapter 1, Sec. 1.4 and Fig. 1.11).

7.5.2 The Position of E.S.R. Absorptions; the *g* Factor

We know from Sec. 7.1.2 that the spin energy levels of an electron are separated in an applied magnetic field, B_0, by an amount:

$$\frac{\Delta E}{h} = \frac{g\beta B_0}{h} \quad \text{Hz} \tag{7.16}$$

where β is the Bohr magneton (9.273×10^{-24} J T^{-1}) and g the Landé splitting factor. A resonance absorption will thus occur at a frequency $\nu = \Delta E/h$ Hz. From Eq. (7.16) we see that the position of absorption varies directly with the applied field and, since different e.s.r. spectrometers operate at different fields, it is far more convenient to refer to the absorption in terms of its observed g value. Thus, rearranging Eq. (7.16) we have:

$$g = \frac{\Delta E}{\beta B_0} = \frac{h\nu}{\beta B_0} \tag{7.17}$$

and if, for example, resonance were observed at 0.34 MHz in a field of 9506.690 T, it would be reported as resonance at a g value of 2.0023. This very precise figure is the g factor for a free electron (rather than the slightly approximate value of two given by putting $L = 0$ in Eq. (5.28)), but it is a remarkable fact that virtually all free radicals and some ionic crystals have a g factor which varies only some ± 0.003 from this value. The reason for this is essentially that in free radicals the electron can move about more or less freely over an orbital encompassing the whole molecule (as we shall see in the next section) and it is not confined to a localized orbital between just two of the atoms in the molecule. In this sense it behaves in very much the same way as an electron in free space, having $L = 0$.

Some ionic crystals, on the other hand, have very different g factors, values between about 0.2 and 8.0 having been reported. The difference here is that the unpaired electron is contributed by, and 'belongs' to, a particular atom in the lattice, usually a transition metal ion. Thus the electron is localized in a particular orbital about the atom, and the orbital angular momentum

(L value) couples coherently with the spin angular momentum, giving rise to a g value consistent with Eq. (5.28).

Nonetheless, many ionic crystals show a g factor very close to the free electron value of 2; this may come about in two ways:

1. The ion contributing the electron may exist in an S state (that is $L = 0$). For example, the ground state of Fe^{3+}, in which five d electrons are unpaired (that is $S = \frac{5}{2}$, $2S + 1 = 6$), has zero orbital momentum. Thus $L = 0$, $J = S + L = S$, and the term symbol is $^6S_{5/2}$ (cf. Chapter 5). Since $J = S$, $g = 2$ (Eq. (5.28)).
2. The electric fields set up by all the ions in a crystal may be sufficiently strong to *uncouple* the electron's orbital momentum from its spin momentum—i.e. coherent Russell–Saunders coupling breaks down and, on the application of a magnetic field, the electron spin vector precesses *independently* about the field direction. Thus the value of L is immaterial and the g factor reverts to two. On the other hand, if the internal crystal field is weak or if the paramagnetic electron is well shielded from the field (e.g. as in a rare earth metal, where the relevant electron orbit is buried deep within outer electron shells), L and S couple to produce a resultant J which itself precesses about the applied magnetic field, and g is given by Eq. (5.28). Intermediate cases also occur where L and S are only partly uncoupled, the residual orbital contribution to the energy giving rise to a g value not easily predictable theoretically.

7.5.3 The Hyperfine Structure of E.S.R. Absorptions (Electron–Nucleus Coupling)

In e.s.r. spectra we must distinguish between two kinds of multiplet structure; there is *fine structure*, which occurs only in crystals containing more than one unpaired electron spin, and *hyperfine structure*—a smaller effect—which arises when an unpaired electron can get close to a nucleus with non-zero spin. We shall deal with the latter in this section and leave until Sec. 7.5.5 our discussion of fine structure.

It is the interaction of the magnetic moment of the unpaired electron with those of any surrounding nuclei having non-zero spin which gives rise to hyperfine structure. This coupling is exactly analogous to the coupling between nuclear spins discussed in Sec. 7.2.2 earlier—indeed, the bulk of that discussion and Fig. 7.12 apply exactly to the electron–nucleus coupling if we label the nucleus as A and the electron X. For simplicity we shall limit our treatment here to nuclei of spin $\frac{1}{2}$ which will split electron resonances into doublets. If more than one nucleus can interact with a given electron, the result can be predicted using the 'family tree' method discussed in Sec. 7.2.3 and Fig. 7.16.

Electron–nucleus coupling constants are very much bigger than those for nucleus–nucleus interactions, firstly because an electron can approach a nucleus more closely than can another nucleus and secondly because the electron's magnetic dipole is some 1000 times larger than that of a nucleus. Thus in the hydrogen atom the electron resonance shows two equal lines with a separation of about 0.05 Tesla. We have seen that a bulk field of 0.34 T is equivalent to a frequency of about 9500 MHz, so 0.05 T is some 1400 MHz, which is an enormous coupling compared to the largest nucleus–nucleus coupling of about 2 kHz.

For most organic molecules with an unpaired spin the coupling constants are of order 10^{-4}–10^{-3} tesla (2–20 MHz); these are smaller than in the hydrogen atom because an unpaired electron in a molecule is never confined to just one nucleus and seldom even to one bond, but can move over several bonds with relative ease, spending only part of its time at any one nucleus. Another way to look at this is in terms of *electron density*. In the hydrogen atom the electron density of the unpaired electron is 1—the electron is in the atom and nowhere else. To a

good approximation the magnitude of the coupling constant is directly related to the electron density, and we can write:

$$A = R\rho \tag{7.18}$$

where A is the coupling constant, ρ the electron density, and R the intrinsic coupling for unit density. For hydrogen, $\rho = 1$ and A, we have seen, is 0.05 T; thus $R = 0.05$ T. Figure 7.26 shows, at the bottom, the e.s.r. spectrum of the methyl radical, $\cdot CH_3$. Remember that, since this is a derivative spectrum, the actual centre of each peak should be measured at the point where the slope is zero, i.e. where the downward-sloping line crosses the x axis. However, the height of the maximum of each point above the x axis is a good approximation to the intensity of the normal, non-derivative, line in the spectrum, and it is clear that Fig. 7.26 arises from a 1 : 3 : 3 : 1 quartet. Intuitively we would expect the electron to spend an equal amount of time on each hydrogen (the electron density at each should be identical), and so to couple equally to all three; this would result in the electron's resonance being split into a 1 : 3 : 3 : 1 quartet, as shown by the family tree in the top part of the figure. Clearly the $\cdot CH_3$ spectrum below corresponds exactly to this pattern. The separation between the lines—the coupling—is found to be about 2.3 millitesla (mT), and so we can use Eq. (7.18) to calculate $\rho = A/R = 0.0023/0.05 = 0.046$. Thus we have the electron density at each hydrogen to be 0.046, or 4.6 per cent, and so we know

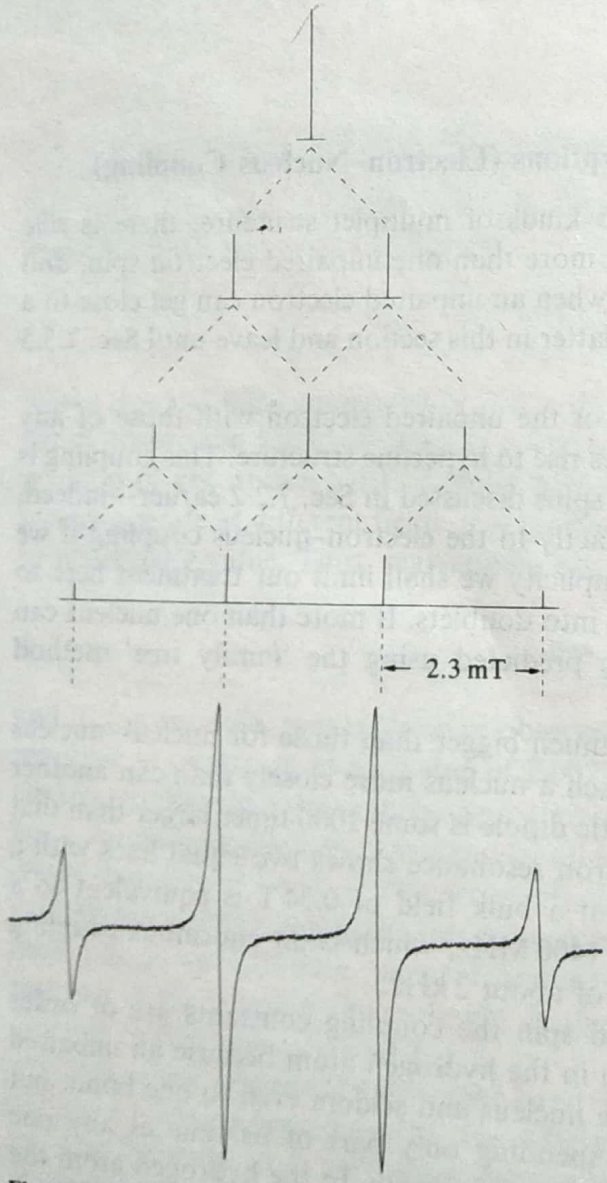

Figure 7.26 The e.s.r. spectrum of the methyl radical, $\cdot CH_3$, and the 'family tree' of couplings which produce it.

that the electron spends nearly 5 per cent of its time at each hydrogen and the remaining $100 - 3 \times 4.6 \approx 86$ per cent on the carbon.

A slightly more complex example is shown in Fig. 7.27, which illustrates the e.s.r. spectrum of the benzene radical, $\cdot C_6H_6$. Here we see a septet of lines, indicating equal coupling to all six hydrogens; the coupling constant is 0.38 mT, and we calculate $\rho = 0.38 \times 10^{-3}/0.05 \approx 7.6 \times 10^{-3}$. There are six hydrogens with this electron density, making a total of $6 \times 7.6 \times 10^{-3} = 0.046$, or nearly 5 per cent in total. Clearly the remaining 95 per cent of the electron's time is spent equally on the six carbon atoms, making nearly 16 per cent on each. Note that Figs 7.26 and 7.27 are drawn to a very different horizontal scale.

If the electron can couple to more than one set of nuclei, the pattern becomes more complicated, but can be rationalized by using the family tree again. The spectrum of the naphthalene radical is shown in Fig. 7.28. This complex pattern can be easily understood once it is realized that, because of the symmetry of the molecule, there are only two different sorts of hydrogen—the positions are numbered in the conventional sense in the molecular picture drawn in the diagram. A moment's thought will make it clear that hydrogens 1, 4, 5, and 8 are an equivalent set, as are hydrogens 2, 3, 6, and 7. The electron couples to the latter group with $A = 1.83 \times 10^{-4}$ T and, since there are four hydrogens, the pattern will be a 1 : 4 : 6 : 4 : 1 pentet. One such pentet is picked out on the left of the diagram. Because of the other group of four hydrogens ($A = 4.95 \times 10^{-4}$ T), this pentet will itself be split into a 1 : 4 : 6 : 4 : 1 pentet; finding these in the spectrum is left as an exercise for the student, but the centre of one other pentet has been picked out on the diagram to help. The assignment of the 1.83×10^{-4} T coupling to the 2, 3, 6, and 7 hydrogens is not made arbitrarily, of course. It can be checked by substituting one or more of the hydrogens with a non-spinning nucleus (e.g. a methyl group), or with a deuterium atom (which has a smaller coupling constant to the electron because of its different magnetic moment), and noting how the spectrum changes.

This use of e.s.r. techniques allows us to build up a qualitative picture of the electron distribution within a molecule which may help, for instance, in understanding chemical reactions—a positively charged reactant will plainly tend to attack that part of a molecule where the electron density is greatest, and vice versa. However, the observed results are not always in good quantitative agreement with the predictions of the molecular orbital theory, particularly for situations where simple molecular orbital theory predicts zero electron density at some points within a molecule—often coupling is observed to occur with nuclei at these points. For instance,

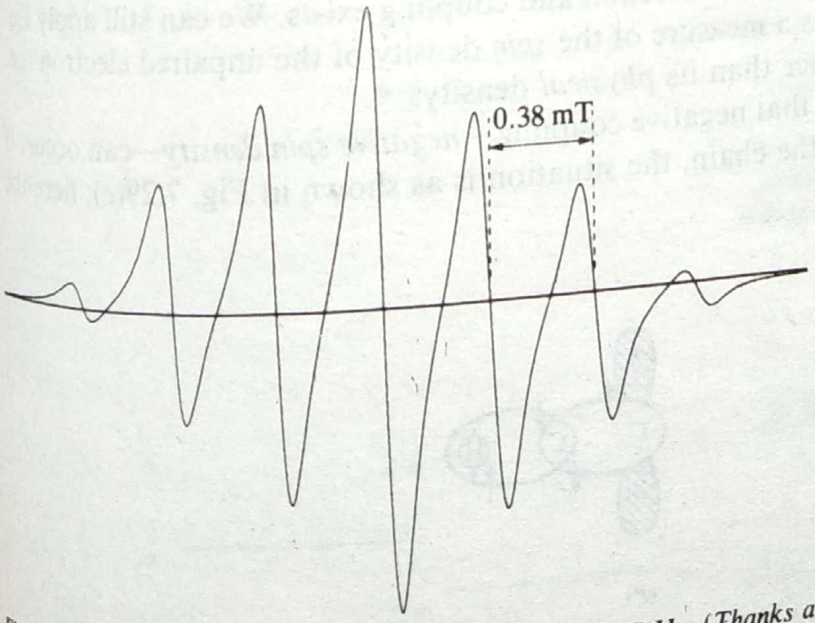

Figure 7.27 The e.s.r. spectrum of the benzene radical, $\cdot C_6H_6$. (*Thanks are due to Dr A. Whitwood of the University of York for this spectrum.*)